UNRAVELLING THE GORDIAN KNOT AT THURSDAY'S GOSSAN

Chris Cairns, Hamish Forgan, Michael Agnew, Stephen Johnson, Jennifer Murphy and Greg Corbett

Key Words: Porphyry copper, gold, Mount Stavely Volcanic Complex, Thursday's Gossan prospect, Lachlan Fold Belt, Victoria, vein copper, polymetallic mineralisation, potassic alteration, phyllic alteration, sulphur isotopes, SWIR

INTRODUCTION

The Thursday's Gossan porphyry, polymetallic-vein and epithermal copper-gold-silver deposit occurs within the Mount Stavely Volcanic Complex of the Grampians-Stavely Zone, western Victoria (Figure 1). Host sequence serpentinite, turbidite sandstone to mudstone (and rare shale), hyaloclastite andesite, dacite and minor basalt lavas have been cut by north- and northwest-trending faults which are intruded by subvolcanic stocks and dykes of diorite, dacite and tonalite. Minor more mafic monzogabbro intrusions and lamprophyre dykes also occur and may have influenced the metallogenic evolution of the multi-phase intrusion / mineralising system.

The Cambrian Stavely Magmatic Arc is interpreted to have formed proximal to a subduction zone located on the eastern continental margin of Gondwana. At a regional scale, the host volcano-sedimentary package includes the Williamsons Road Serpentinite and the Glenthompson Sandstone, which have been intruded / overlain by members of the Stavely Volcanic Arc including the Fairview Andesite Breccia, the Narrapumelap Road Dacite, the Nanapundah Tuff and the Towanway Tuff (Cayley et al 2018, Stuart-Smith and Black 1999).

These units have been intruded by the Lalkaldarno Porphyry, Victor Porphyry, Buckeran Diorite, Bushy Creek Granodiorite and the Thursday's Gossan intrusive complex.

The Thursday's Gossan deposit is located between the regionally extensive northwest- to west northwest-trending Escondida and Mount Stavely faults, strike-slip structures which were active during both the Delamerian and Benambran orogenies (Schofield ed., 2018).

At a regional scale, the interaction of the NS and NW structures in an oblique sinistral strike-slip sense of movement has resulted in left 'steps' of the NS structures where they intersect the NW structures. Commonly, the basal serpentinite can be seen in the magnetic data to be structurally thickened in proximity to these 'steps'. Locally, the Mount Stavely structure displays a clear flexure in the vicinity of Thursday's Gossan which, in a sinistral stress environment, has facilitated a pull-apart dilation into which a series of productive porphyry phases have been intruded (Figure 2).

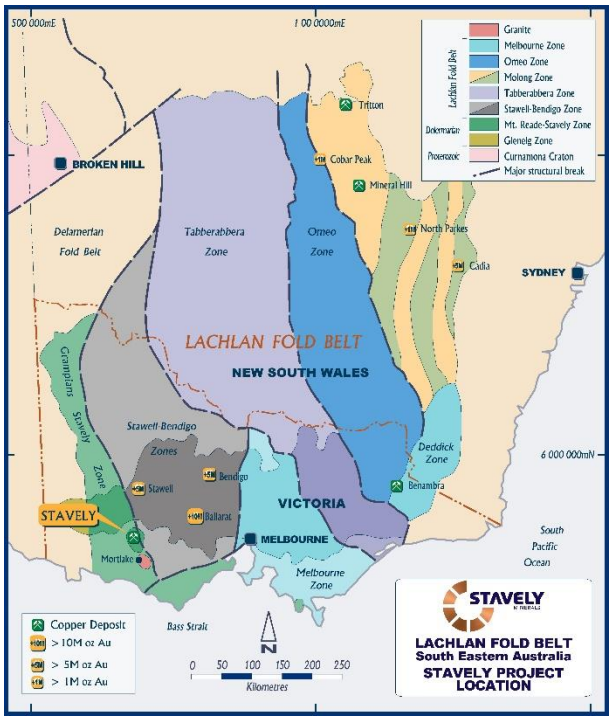

Figure 1. Stavely Project location map.

A focussed drilling campaign by Stavely Minerals, beneath the existing supergene copper resource (28Mt at 0.4% Cu; Cairns et al, 2015) has delineated broad intervals of low-grade copper mineralisation, hosted in early quartz ± magnetite and massive quartz-pyrite veins associated with a high-level multiphase intrusive complex and later structurally-controlled, polymetallic lodes of chalcopyrite ± bornite ± chalcocite ± covellite ± enargite ± tennantite/tetrahedrite that cut across both the intrusive complex and surrounding volcano-sedimentary host rocks.

Stavely Minerals has completed an extensive program of petrological descriptions, short-wavelength infra-red and geochemical analyses on drill core and drill percussion chip samples in order to characterise the host rocks, intrusion history, hydrothermal alteration assemblages and mineralisation, including:

- >30,000 spectral measurements from a TerraSpec Halo Mineral Identifier
- 219 samples for sulphur isotopic analysis of pyrite, chalcopyrite, bornite and anhydrite
- 194 thin sections for petrological analysis
- 124 samples for whole rock multi-element lithogeochemistry
- >23,000 samples for gold and multi-element geochemistry by ALS Laboratories methods AU-AA23 & ME-ICP61.
- 10 samples of intrusions for U-Pb geochronology
- 2 molybdenite samples for Re-Os geochronology

LOCAL GEOLOGY

The Thursday's Gossan deposit is hosted by a deep marine volcano-sedimentary package comprising a basal pervasively serpentinised ultramafic and massive- to thinly-laminated turbidites with medium-coarse terrestrial sandstone bases, grading upward to siltstone / mudstone, volcaniclastic sandstone, volcaniclastic breccia, basalt, hyaloclastite andesite and dacite lava flows (Figure 3).

The volcano-sedimentary package hosts a multiphase intrusion centre ranging in composition from calc-alkaline to sub-alkaline diorite to dacite considered chemically fertile for porphyry-style mineralisation. Emplacement of these intrusions and associated polyphase mineralisation was controlled by movement and subsequent reactivation of the locally expressed North South Fault (NSS), related NW faults, and a NE striking Copper Lode Splay (CLS) (Figure 4). It is likely that a number of parallel and sympathetic structures remain to be identified. Late mineral intrusions genetically-related to the porphyry system were emplaced on a number of these structures before a series of low volume,

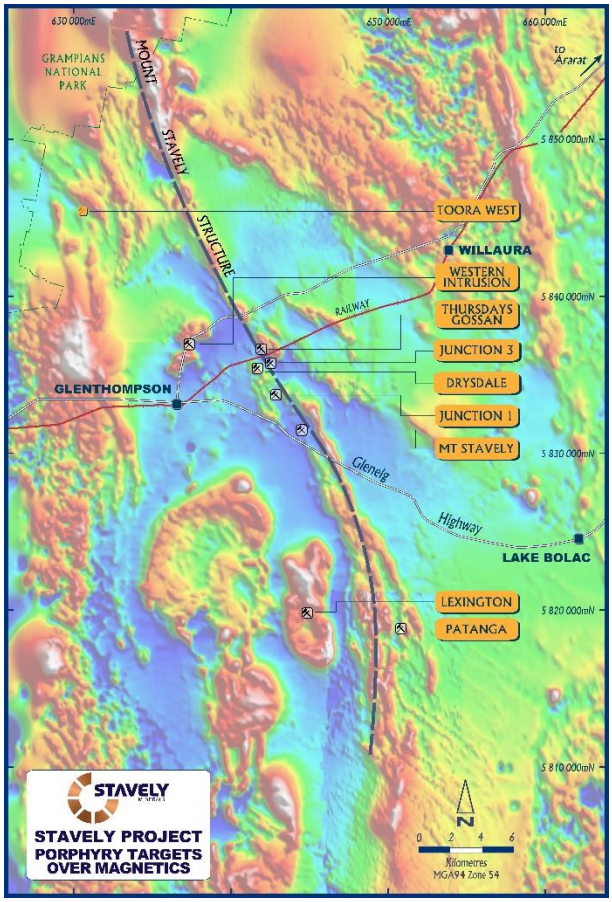

Figure 2. Aeromagnetic image (RTP) showing the Stavely Magmatic Arc and the Mount Stavely Fault.

post-mineral intrusions crosscut the intrusive complex.

Intrusive relationships at Thursday's Gossan are defined based on the observation of: the intensity of veining, alteration, and mineralisation, truncation of veinlets, chilled or flow banded margins and the presence of xenoliths (Lickfold 2002; Sillitoe, 2000). Applying these criteria to rocks at Thursday's Gossan defines intrusions as Pre-Mineral Intrusions, Early Porphyries, Inter-Mineral Porphyries, Late Mineral Porphyries and Post-Mineral Intrusions in the following sequence of emplacement (Figures 5-8):

Pre-Mineral Intrusions

1. Microdiorite Porphyry (MDP)
2. High Phosphorous Microdiorite (HPMD)
3. Early Dacite Porphyry (EDP)

Early Porphyry

4. Victor Tonalite Porphyry (VTP)
5. Quartz Diorite Porphyry (QDP)

Inter-Mineral Porphyry

6. Inferred Porphyry 3 (IP3)
7. Inferred Porphyry 4 (IP4)

Late Mineral Porphyry

8. Late Mineral Dacite (LMD), Late Dacite porphyry (LDP)

Post Mineral Intrusions

9. Monzogabbro (?)
10. Lamprophyre Dyke (LAMP)
11. Lalkaldarno Porphyry
12. LKD Diorite Dyke (LKD)
13. Microgabbro Dyke (MG)

Pre-mineral intrusions include the Microdiorite Porphyry (MDP), the High-Phosphorous Microdiorite (HPMD) and the Early Dacite Porphyry (EDP). The HPMD is characterised by +3,000ppm P and commonly +1.2% Ti. It is enigmatic as it does not have any genetic relationship to any of the other intrusions in the prospect area.

Early porphyry phases include the Victor Tonalite Porphyry (VTP) located in the centre of the large 1km by 4km alteration system and the Quartz Diorite Porphyry (QDP) mainly located in the northern portion of the prospect area and the focus of much of the recent drilling. The QDP is believed responsible for the intense quartz-magnetite porphyry M-style veins (using the classification of Arancibia and Clark, 1996) veining in the apical portions and margins of the QDP, and extending into the HPMD and other host units.

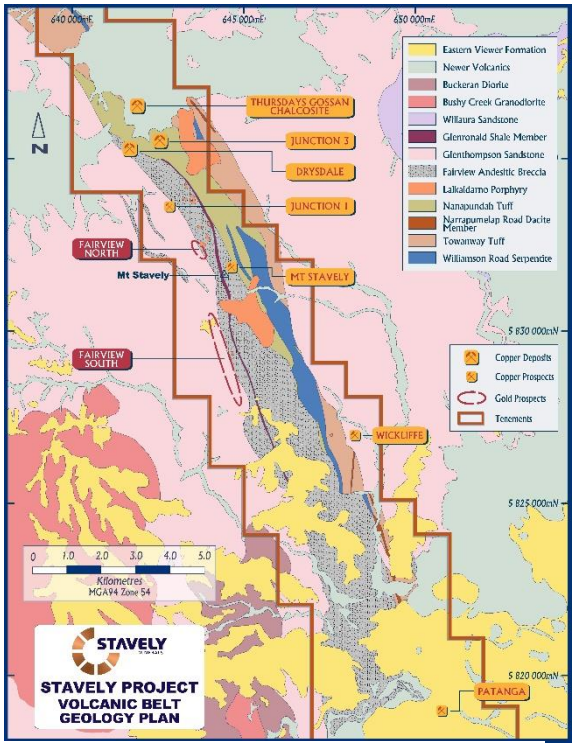

Figure 3. Thursday's Gossan local geology.

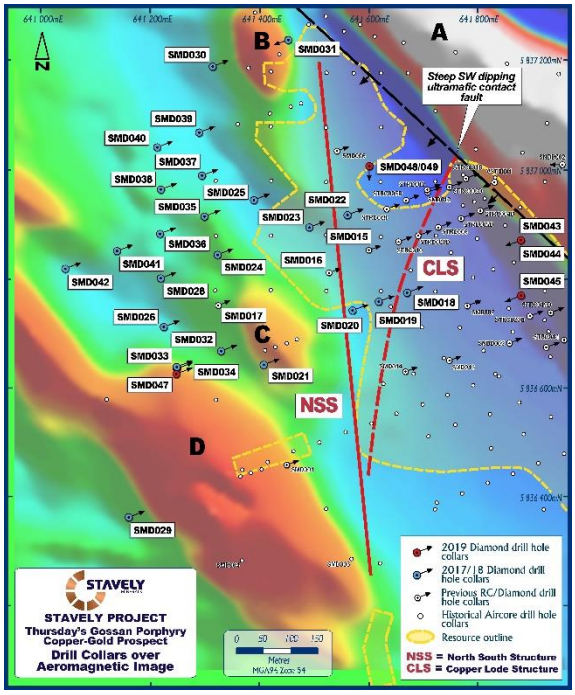

Figure 4. Thursday's Gossan drill hole collars, mineralised structures on RTP magnetic image.

The QDP is cut by a large number of quartz-pyrite porphyry D-style veins (using the classification of Gustafson and Hunt, 1975) inferred to have emanated from an unseen Inferred Porphyry 3 as late-stage veins to that porphyry. These porphyry D veins are then brecciated / reopened and in-filled by later bornite ± chalcocite ± chalcopyrite ± covellite ± enargite ± digenite ± tennantite ± colusite ($Cu_{13}VAs_3S_{16}$) veins (Ashley, 2019) interpreted to be part of a later prograde mineralising event associated with unseen Inferred Porphyry 4.

In total, four porphyry alteration / mineralisation events have been noted and inferred at Thursday's Gossan.

The Late Mineral Dacite cuts all of the preceding intrusions. Post-mineral intrusions include the Cambrian monzogabbro, the lamprophyre dyke and the unaltered / unmineralised Cambrian Lalkaldarno porphyry. The LKD diorite dyke is dated as Devonian (circa 400Ma) and is cut by the undated microgabbro dyke(s). A more extensive discussion of the regional and prospect-scale geochronology is presented in Appendix 1 and is summarised in Figure 7.

Structural Setting

Orientation of the major structures (Figures 4 and 5) at the Thursday's Gossan deposit include;

- Ultramafic Contact Fault (UCF), oriented -60-80°/240° with the Williamsons Road Serpentinite in the footwall and the Mount Stavely Volcanic Complex in the hangingwall
- North South Structure (NSS), trending -80°/260°
- Low Angle Structure (LAS), trending -30°/220° to -50°/260°
- Copper Lode Splay (CLS), trending -60-70°/280°.

Shear sense indicators and 100-200m of apparent offset of the intrusive units indicate that the NSS and LAS are normal-dextral and reverse-sinistral faults respectively – noting that

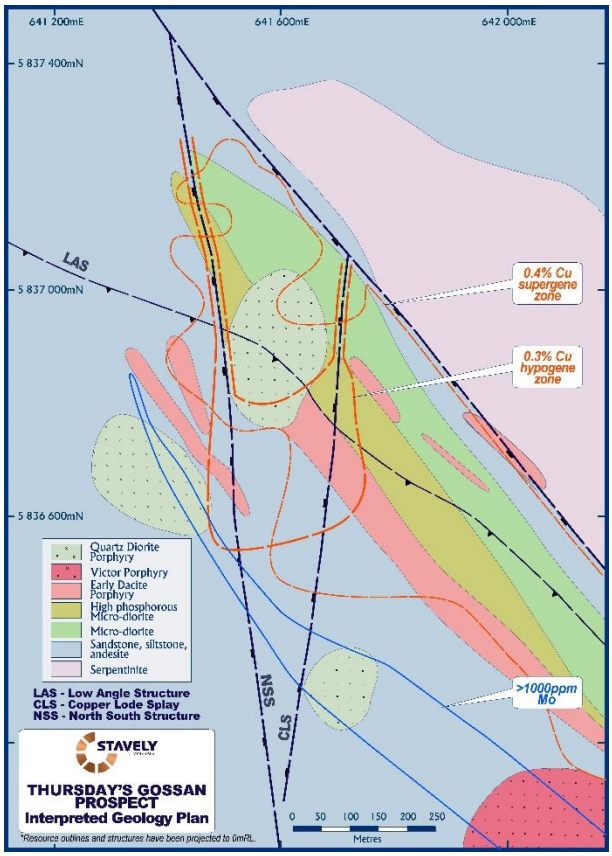

Figure 5. Local geology interpretation showing structures and mineralisation outlines.

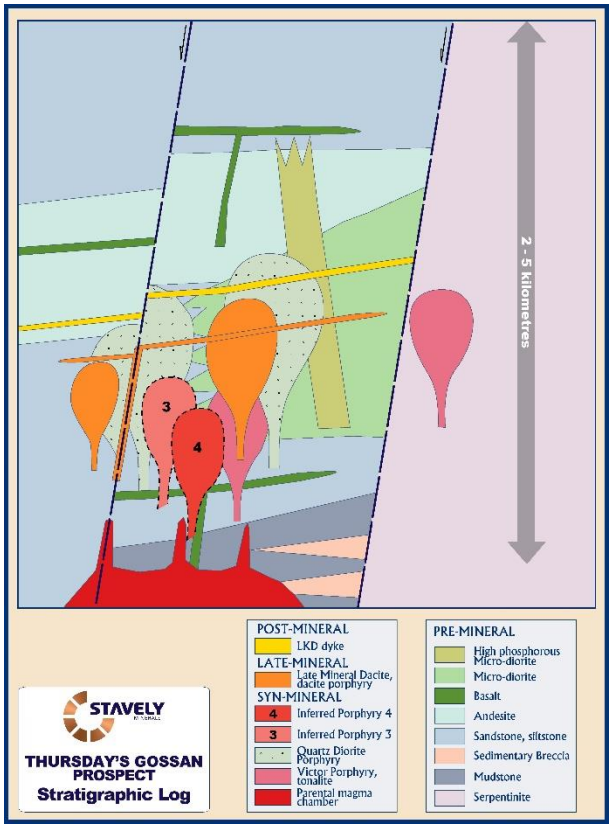

Figure 6. Thursday's Gossan deposit stratigraphy.

this net offset is a combination of differing Cambrian and Devonian stress orientations. There also appears to be a late west block up component to the NSS likely during the Benambran Orogeny. All structures transect the host rock package. Recent drilling has encountered polymetallic lode-style copper-gold-silver mineralisation primarily along the NSS and CLS (Figure 5), with minor mineralisation in the LAS and UMC indicating that the NSS, CLS, UMC and LAS were all active during the emplacement of the intrusive complex and subsequent hydrothermal fluid migration and mineralisation.

The arc-parallel north-oriented structures appear to step across the NW oriented structures and these steps are associated with a structural thickening of the basal serpentinite. This implies a sinistral sense of movement allowing for pull-apart dilation on the NW steps. This pull-apart dilation is interpreted to have provided the space for the porphyry intrusions at Thursday's Gossan.

Mineralisation emplaced into the NE trending CLS fault is interpreted to have occurred during a transient relaxation of the sinistral strike-slip oblique convergence to provide EW extension (Corbett, 2019a).

The LAS was re-activated in the Devonian and hosts the circa 400Ma LKD diorite dyke.

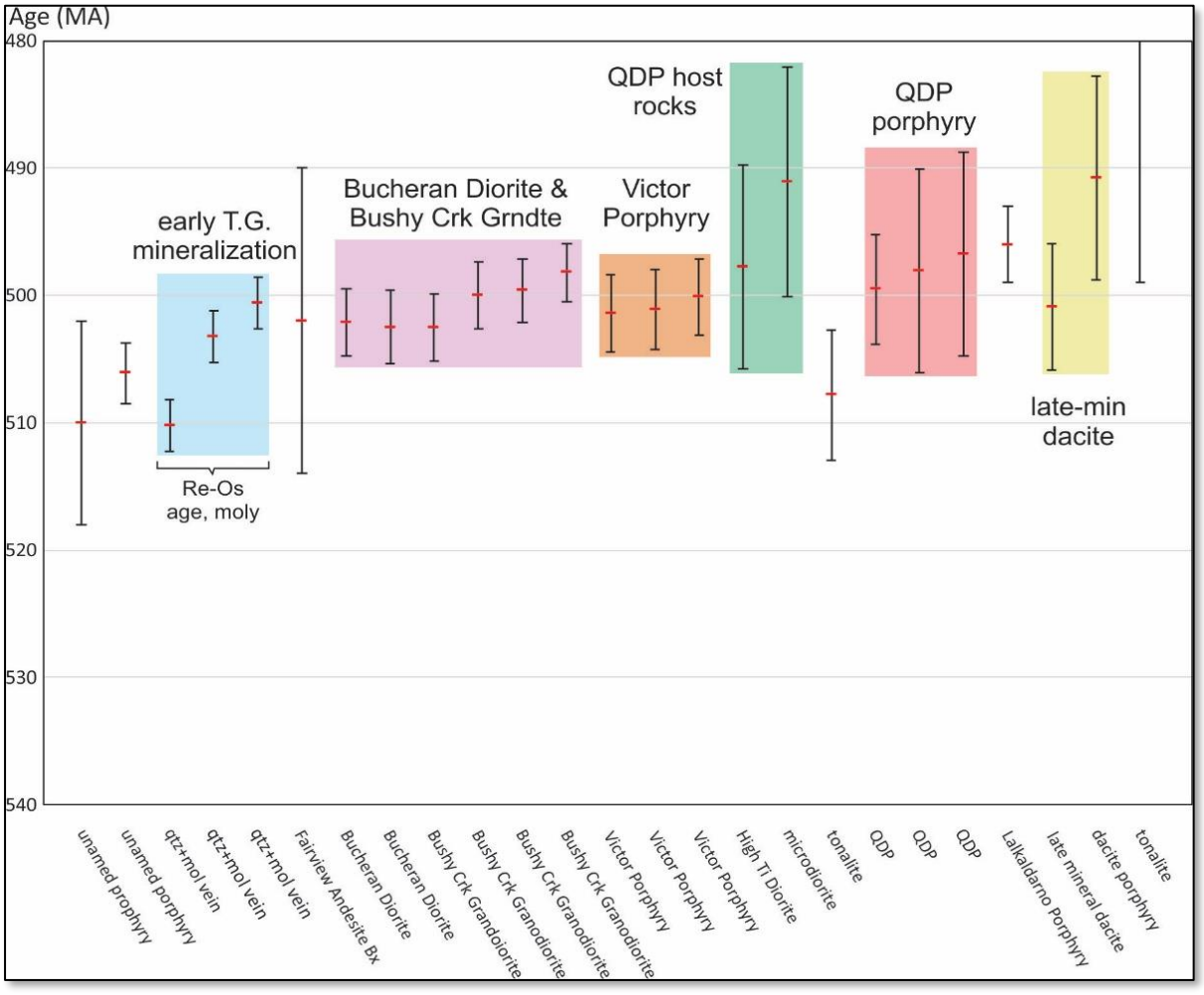

Figure 7. Summary of geochronology from Thursday's Gossan and the surrounding Stavely Belt with error margins. All ages were derived from U-Pb isotopic ratios in zircons, except where indicated. A compilation of data from Stavely Minerals (2018, 2019), Norman (2014, 2015), Lewis et al (2015, 2016) and Bucher (unpublished Ar-Ar date presented in Stuart-Smith and Black, 1999).

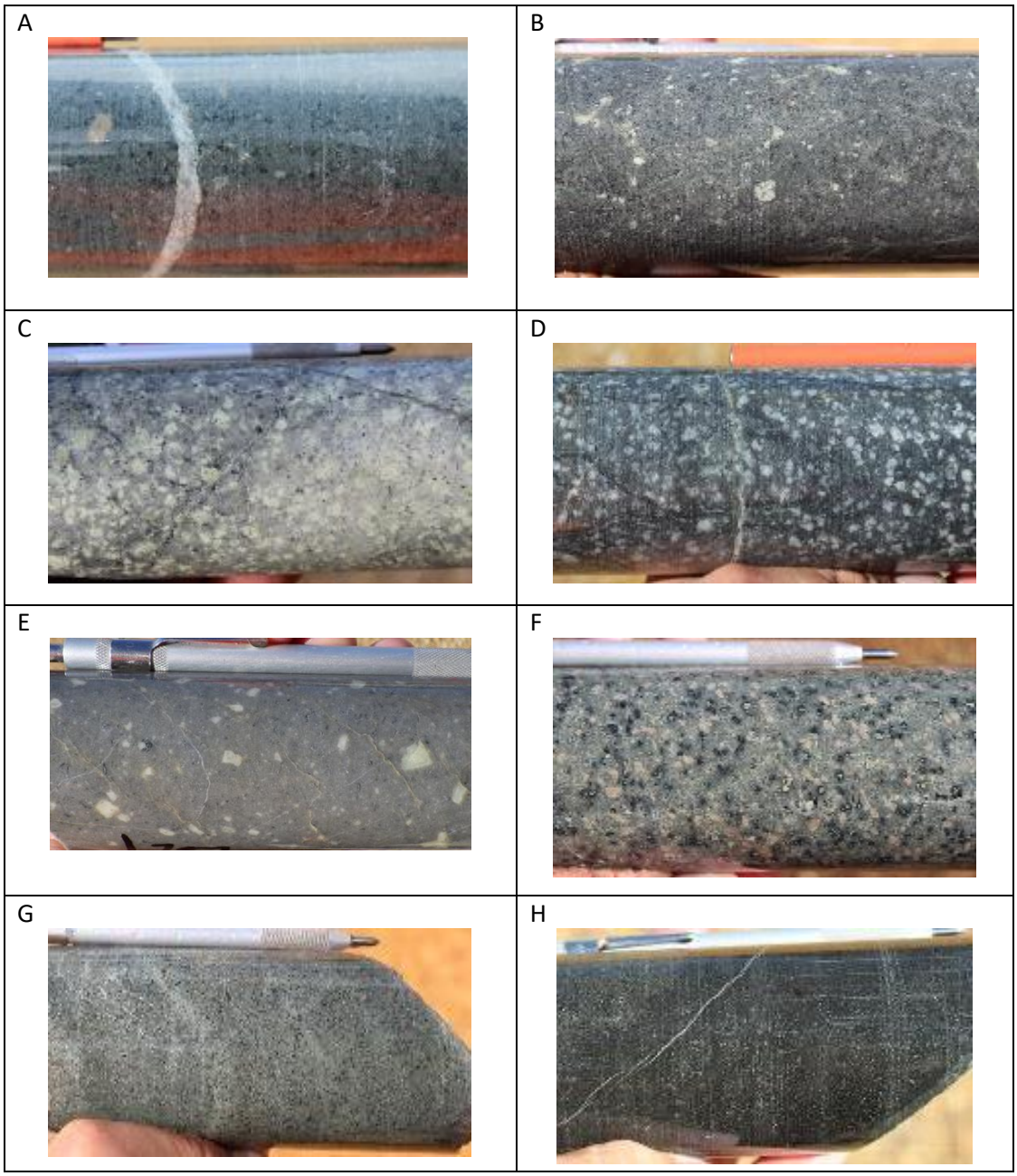

Figure 8. Example photographs and rock descriptions from the Thursday's Gossan Intrusive Complex in order of emplacement; A. Fine grained porphyritic micro diorite. hornblende, plagioclase and quartz phenocrysts in a groundmass of abundant plagioclase and lesser quartz and ferromagnesian material from SMD038 at 285m. B. Fine grained porphyritic high-phosphorous microdiorite. Plagioclase, horneblende, FeTi oxide phenocrysts enclosed in a fine to medium grained groundmass of plagioclase, ferromagnesian material, FeTi oxide and apatite from SMD016 at 316.2m. C. Variable fine to coarse grained porphyritic dacite porphyry (EDP). Phenocrysts of plagioclase, hornblende and occasional quartz eyes within quartzofeldspathic groundmass from SMD024 at 315.8m. D. Coarse grained porphyritic quartz diorite porphyry (QDP). Phenocrysts of plagioclase, hornblende and quartz within an inequigranular groundmass of fine grained intergrown plagioclase and quartz from SMD036 at 462.8m. E. Fine to medium grained porphyritic dacite. Referred to as the Late Mineral Dacite (LMD) in the project area. Fine plagioclase with scattered plagioclase megacrysts, and hornblende in a finer grained quartzofeldspathic groundmass with occasional quartz phenocrysts from SMD041 at 757m. F. Porphyritic Micro diorite referred to as LKD dyke in the project area. Phenocrysts of blocky plagioclase, hornblende, pyroxene and possible pyroxene within a groundmass of fine to medium grained plagioclase and ferromagnesian material from SMD020 at 326.2m. G. Massive, medium grained hornblende microgabbro (MG). Phenocrysts of small blocky plagioclase intergrown with hornblende from SMD020 at 209.2m. H. Microporphyritic lamprophyre. Abundant microphenocrysts of olivine and clinopyroxene, minor alkali feldspar, biotite, clinopyroxene and titanomagnetite from SMD021 at 344.7m.

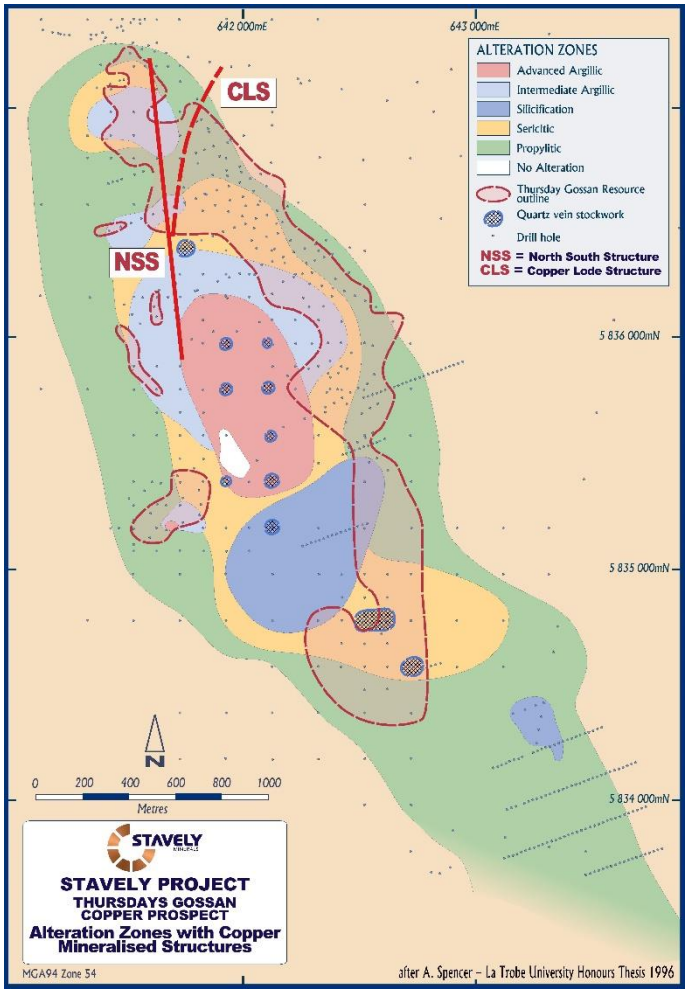

Figure 9. Thursday's Gossan alteration zonation (modified from Spencer, 1996).

HYDROTHERMAL ALTERATION

The intrusive complex at Thursday's Gossan is spatially related to a 1km x 4km NNW trending alteration system comprising silicification, intermediate argillic, argillic, phyllic, sodic and propylitic alteration assemblages originally described by Spencer (1996) and based on PIMA analysis of aircore drill chips (Figure 9). Trace relict and intermittent indications of early potassic alteration in the form of secondary biotite and K-feldspar have been observed (Corbett, 2019a; Ashley 2017-2019). Argillic alteration (described as advanced argillic in Spencer, 1996) occurs as a zone of pervasive kaolinite, montmorillonite and white mica overprinting the upper ~50-100m of the intrusive complex. Intermediate argillic alteration occurs as a 200-300m thick clay zone centred around a southern zone of felsic intrusions referred to as the Victor Tonalite Porphyry (VTP). Structurally-controlled advanced argillic alunite and vuggy silica have been observed at shallow depths (<150m) in the UMC structure. The alteration transitions vertically and laterally along a number of key structures including the NSS and CLS where moderate pyrophyllite and intense sericite alteration occurs (Figure 10b). This strong phyllic alteration assemblage remains open to the south and at depth. Sodic alteration is observed as pervasive albite replacement of plagioclase within the QDP and less well developed within the surrounding EDP, MDP, HPMD and andesite volcanic host rocks. Phyllic alteration occurs as a broad zone of both pervasive and vein selvedge sericite, pyrite and chlorite broadly within a few hundred meters of the intrusive complex. A more intense phyllic assemblage occurs as pervasive sericite alteration within and surrounding faults and as selvages to the very common porphyry D-style veins (using the classification of Gustafson and Hunt, 1975) throughout the deposit. Propylitic assemblages occur as disseminated and vein hosted epidote, chlorite, carbonate and minor actinolite-magnetite alteration both within and extending beyond the intrusive complex.

Analysis of the spatial distribution of the 2200nm SWIR absorption feature in porphyry systems has demonstrated that lower wavelengths correspond to the strongest and most proximal zones of phyllic alteration and are interpreted to reflect a relatively undiluted fluid of magmatic origin (eg. Halley et al. 2015). Systematic analysis of drill core samples at Thursday's Gossan via ASD TerraSpec Halo SWIR Mineral Identifier demonstrates a continuous zone of low wavelength 2200nm absorption features along the NSS and a ~150m zone immediately east of the NSS in association with a logged zone of strong sericite alteration (Figure 10b).

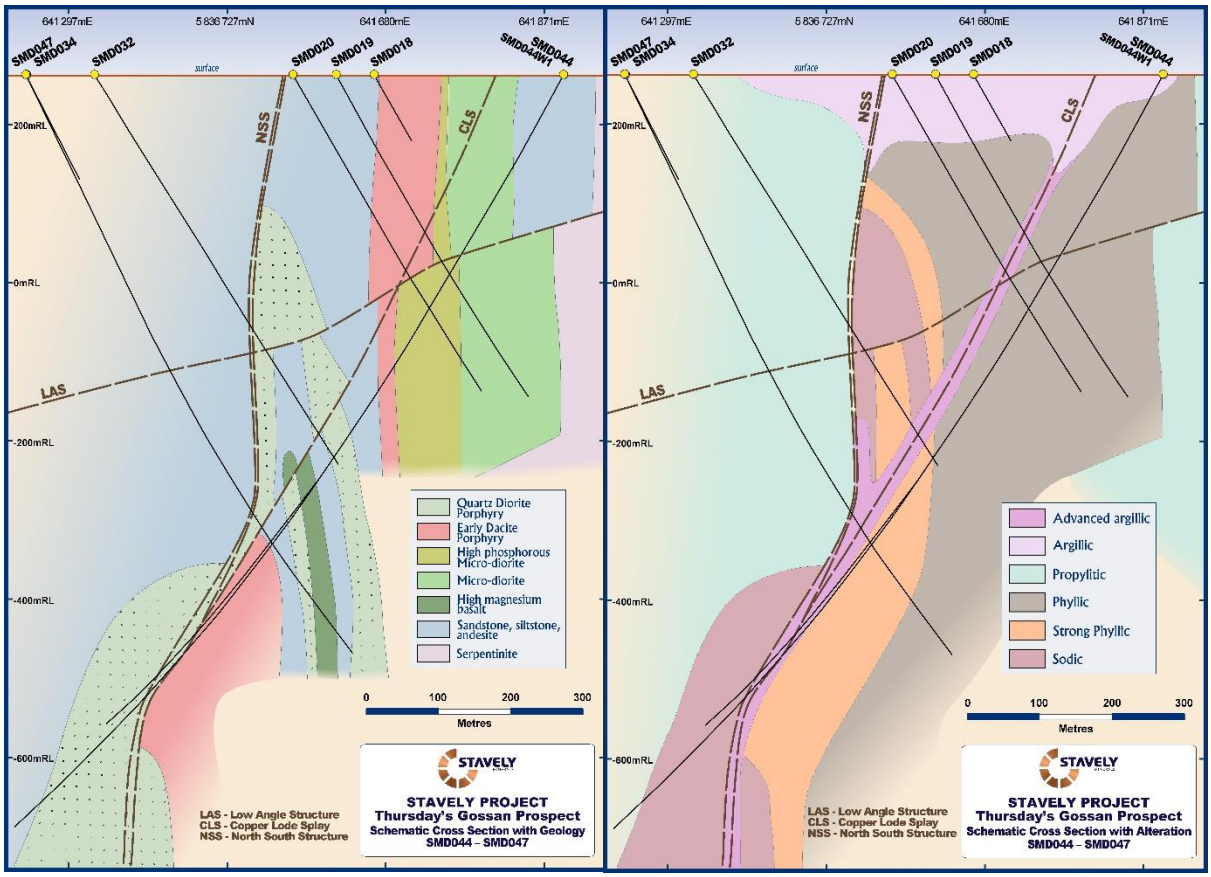

Figure 10. Thursday's Gossan drill section showing (a) geology and mineralised structures on the left and (b) alteration mineral assemblages on the right.

GER control diagrams from multi-element geochemical data further support macroscopic and thin-section analysis indicating a combination of kaolinite, muscovite, albite and chlorite being the most volumetrically significant alteration minerals found throughout Thursday's Gossan (Ashley, 2017-2019; Stanley & Madeisky, 1996; Figure 11).

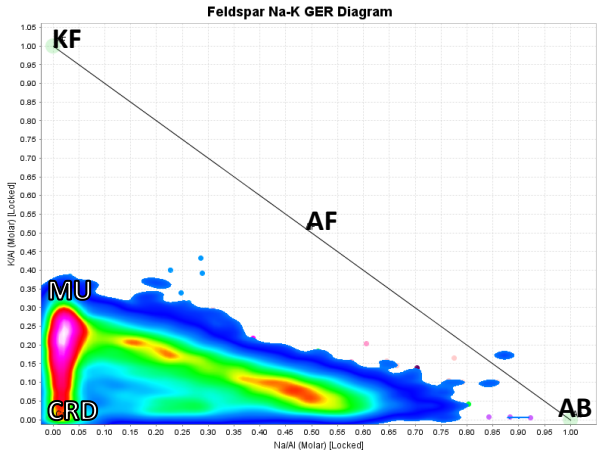

Figure 11. Thursday's Gossan Feldspar Na-K GER density diagram after Stanley & Madeisky, 1996. "KF" orthoclase,"MU" muscovite,"AB" albite, "CRD" cordierite, "AF" Alkali feldspar control line. Samples demonstrate dominant muscovite and albite alteration assemblages.

MINERALISATION AND VEINING

Multiple porphyry intrusions and associated hydrothermal alteration and veining events at Thursday's Gossan has resulted in polyphase temporal overprinting of alteration assemblages and mineralisation styles across the deposit. Broad low-grade copper-gold mineralisation typical of porphyry deposits (eg. Sinclair, 2007) surrounds the intrusive complex as both disseminated and porphyry D vein-hosted quartz-pyrite ± chalcopyrite. Very common massive early pyrite veins occur as a subset of porphyry D veins that extend from within the intrusive complex outwards to the ultramafic contact. Low-grade molybdenum occurs within a sub-set of early quartz A veins extending a short distance from the QDP

intrusions. Narrower (2-40m) zones of later magnetite-hematite-chalcopyrite ± bornite ± hypogene chalcocite mineralisation have been observed within and proximal to both the UMC, CLS and NSS faults zones. Similar hydrothermal alteration and sulphide mineralisation occurs as disseminations and clots in porous hydrothermal breccias and in coarser grained sandstone units. Some of the more intermediate to mafic andesite to high-Mg basalt host units appear to be locally preferentially mineralised. Carbonate base-metal style epithermal Au mineralisation, as defined by Corbett and Leach (1998), occurs as veins of carbonate-pyrite ± galena ± sphalerite ± chalcopyrite, sometimes with appreciable gold, occurs as a peripheral halo to the mineralised volume within the surrounding host rocks. Gold, where noted, occurs as electrum (Ashley, 2018).

Polymetallic lode-style mineralisation is characterised by early, well-developed pyrite-rich porphyry D veins up to several metres thick cut by later bornite ± chalcocite ± chalcopyrite ± covellite ± enargite ± digenite ± tennantite ± colusite which display complex crosscutting temporal relationships (Figure 13E). This style of mineralisation is contained within the NSS, CLS, LAS and UMC structures from as shallow as 65m below surface to at least a kilometre depth with an apparent southerly plunge in the plane of the steep NSS and CLS structures (Figure 12).

Drill hole SMD044 intersected a broad low-grade copper mineralisation within which the higher-grade structurally-controlled copper-gold-silver mineralisation occurs as:

- 952m at 0.23% copper from 11m drill depth, including
  - 10m at 2.43% copper, 0.30g/t gold and 11g/t silver in the CLS
  - 38.3m at 1.59% copper, 0.27g/t gold and 8g/t silver in the NSS, and
  - 18m at 3.62% copper, 0.28g/t gold and 15g/t silver in the NSS (daughter wedge drill hole to SMD044)

Supergene enrichment during Tertiary weathering contributes economically significant fracture, vein-hosted and secondary chalcocite coatings to hypogene sulphide within the upper 80-100m of the deposit and overprints all other mineralisation styles.

A complex series of porphyry-related hydrothermal alteration events and veins have been observed at Thursday's Gossan. Analysis of these veins within the well-described porphyry model (eg. Corbett 2019, Sillitoe 2010, Wilson 2003) suggests the deposit is characterised by a series of overprinting prograde and retrograde porphyry style vein sets.

Early 1-20mm wide inequigranular quartz veins occur without alteration selvages and occasionally contain minor chalcopyrite-pyrite and/or molybdenite. These veins often occur disjointed and display variable watery to wormy textures indicating early formation during emplacement of the QDP. These veins are interpreted to represent porphyry A-style veins (using the classification of Gustafson and Hunt, 1975) (Figure 13A, 13I).

The earliest quartz-magnetite ± minor chalcopyrite/actinolite veins occur as wispy 0.5-2mm quartz veinlets with magnetite aggregates, followed by 2-7mm wide quartz veins with 'railroad track' magnetite margins and later, well developed up to >500mm wide laminated quartz magnetite veins all developed within close proximity (~100m) to the upper margins of the QDP. These veins merge into aplite vein dykes along the intrusive margin of the QDP and emplaced proximal to the QDP cupola. These veins are interpreted to be porphyry M-style veins (using the classification of Arancibia and Clark, 1996) and are analogous to those reported by Wilson (2003) at the Cadia Ridgeway porphyry deposit (Figure 13B, C, D and H).

Well-developed quartz-pyrite and pyrite veins up to several metres' width with distinct and often asymmetric sericite selvages occur within the NSS, CLS, LAS and on prominent E-W trending structures

extending outwards to the UMC structure. Thursday's Gossan displays an unusual abundance of these very large porphyry D veins. The asymmetry of the sericite selvages is interpreted to reflect wider hanging wall and narrower footwall alteration haloes to the porphyry D veins. Pyrite is variably brecciated and in-filled with later chalcopyrite, bornite and other copper sulphides. Open spaces (potentially where anhydrite has been hydrated to gypsum and dissolved) are often observed hosting later low-temperature banded cryptocrystalline silica infill which may indicate a significant cooling / uplift over the duration of the hydrothermal system. These veins are interpreted to represent structurally-controlled late-stage porphyry D-style veins (using the classification of Gustafson and Hunt, 1975) (Figure 13E).

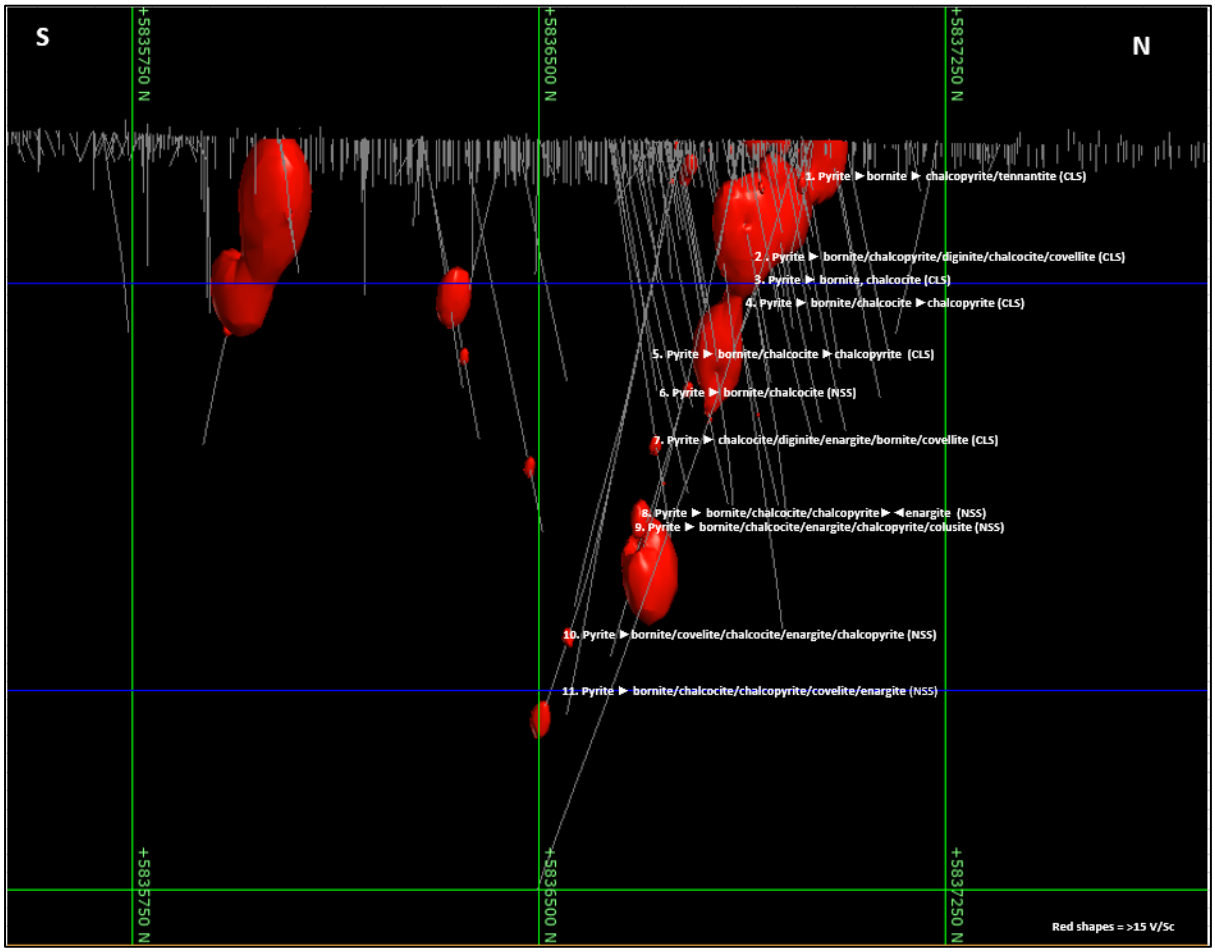

Figure 12. 3D section of Thursday's Gossan which demonstrates a southerly plunging zone of V/Sc > 15 (red bodies). White labels indicate sulphide mineralogy along the NSS and CLS. "►"indicates an observed crosscutting relationship and sulphides are listed in order of abundance for each subsequent

Finer 1-4mm wide pyrite quartz veins, more akin to the 'typical' porphyry D veins, with 5-40mm wide sericite alteration selvages occur dispersed both within and extending well beyond the intrusive complex. These veins are interpreted to also represent porphyry D veins (Gustafson and Hunt, 1975; Corbett, 2017, 2018 and 2019) (Figure 13C & 13G).

A series of 1-100mm wide polymetallic sulphide veins occur within portions of the NSS and CLS with an apparent southerly plunge. These veins occur crosscutting the earlier well-developed pyrite veins and are associated with a short-wavelength sericite, pyrophyllite and dickite assemblage indicative of advanced argillic alteration derived from the reaction of low pH fluids with the wall rocks. Copper sulphide species within the NSS and CLS faults demonstrate a significant generalised zonation with depth and distance from the interpreted source intrusion; enargite ± tennantite ± tetrahedrite ±

colusite ➔ bornite ± chalcocite ± covellite ± digenite ➔ chalcopyrite-bornite ➔ chalcopyrite ➔ sphalerite from deep and proximal to shallow and distal (Figure 12). This change in assemblage with depth is interpreted to reflect complex overprinting relationships associated with changing pH and

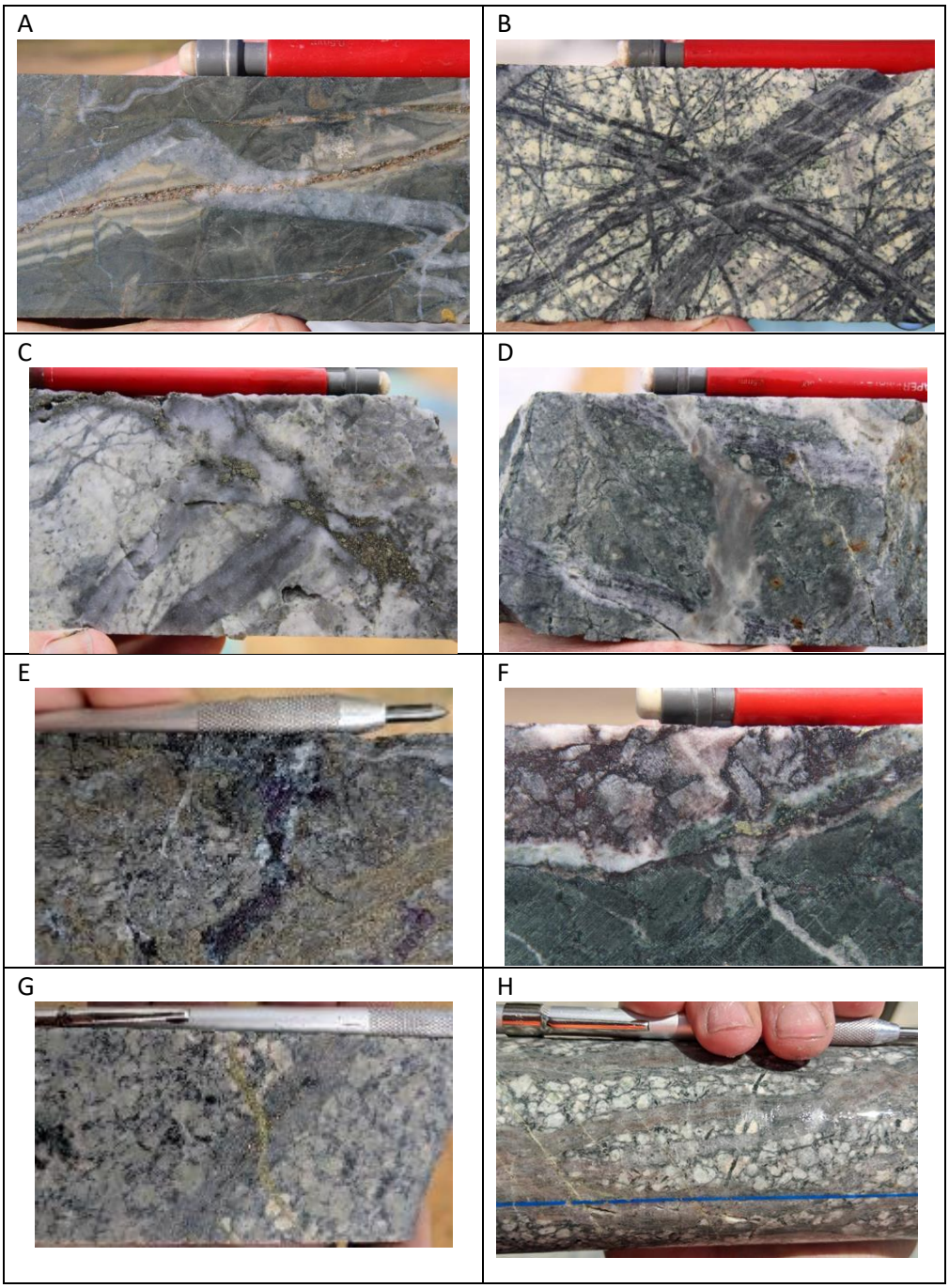

Figure 13. Core photos showing vein crosscutting relationships observed at Thursday's Gossan. A .D vein crosscutting wormy A vein, DDH SMD026 599.1m B. Sheeted and stockwork banded quartz-magnetite overprinted by late phyllic alteration, SMD015, 132.7m. C. A-M veins cut by a pyrite D vein, DDH SMD019, 156.5m. D. Aplite dyke cuts quartz-magnetite veins with actinolite alteration, SMD025, 424.8m. E. Bornite-chalcocite-covelite-tennantite-tetrahedrite veining crosscuts pyrite D veins, SMD044, 924.2m. F. Chlorite-magnetite altered high-Mg basalt with chalcopyrite-bornite cut by anhydrite which is brecciated and infilled with specularite matrix, DDH SMD044, 669.8 m. G. D vein crosscut by epidote veinlet, DDH SMD044W1, 1093.8m. H. Aplite dyke with porphyry A/M veins from DDH SMD041, 568m

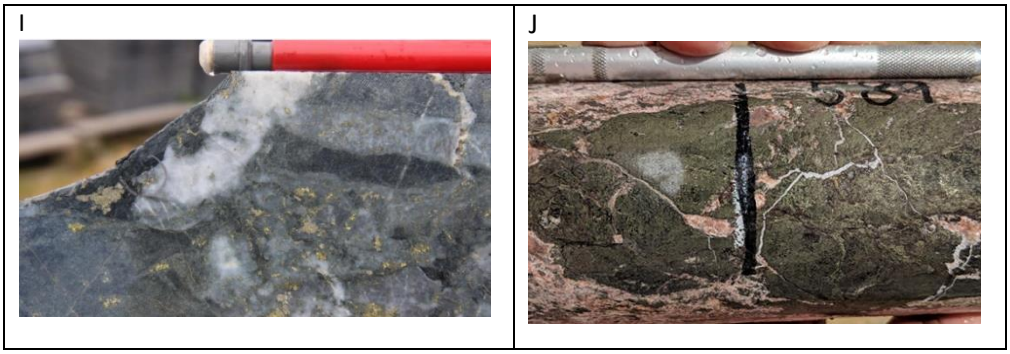

Figure 13 (cont.) I. Porphyry A vein overprinted by Fe-poor, white sphalerite typical of carbonate base metal epithermal Au mineralisation, DDH SMD026, 364.9m. J. Anhydrite/gypsum vein with clot of chalcopyrite, DDH SMD044, 589m, modified from Corbett (2019).

fluid temperature as the fluid moves away from a porphyry source and evolves by cooling, dissociation and mixing (Corbett, 2019a). The general spatial variation in copper sulphide species is complicated by the polyphasal nature of mineralisation and the temporal / spatial effect on a waxing and waning of the hydrothermal system over time.

Common 1-250mm wide anhydrite veins with variable pyrite, chalcopyrite, hematite, specularite and magnetite are observed at depth within 50-200m distance of the NSS and appear to be increasing in intensity at depth and to the south. Two variants of these veins are identified, one with sericite selvages and one without, however the timing relationship between these styles remains enigmatic (Figure 13F & 13J). The anhydrite veins without sericite selvages more commonly contain chalcopyrite, magnetite and hematite and are interpreted to be part of an early porphyry prograde vein event. The anhydrite veins with sericite selvages are interpreted to be part of a late porphyry vein event and are considered a variant of the porphyry D veins. Crosscutting relationships are observed in both directions and may be related to at least two unseen porphyry intrusions.

Carbonate quartz ± galena ± sphalerite ± gold veins occur widely and sporadically distributed in the periphery to the mineralised volume within the surrounding host rocks. Sphalerite occurs as brown, white and grey varieties (Figure 13I).

Analysis of the crosscutting relationship of these veins sets within the well-described framework of porphyry systems (Gustafson & Hunt, 1975; Corbett, 2019b; Sillitoe, 2010; and Wilson, 2003) identifies at least three cycles of prograde and retrograde veins developed in the area of current interest (Figure 13A-I). Observed crosscutting porphyry style veins include;

- Porphyry A veins crosscut by porphyry D veins (Figure 13A).
- Aplite vein dykes and porphyry M veins crosscut by epidote veins (Figure 13H).
- Porphyry D veins crosscut by epidote veins (Figure 13G).
- Porphyry M veins crosscut by porphyry D veins (Figure 13C).
- Porphyry M veins crosscut by aplite vein dykes (Figure 13D).
- Porphyry D veins crosscut by polymetallic mineralisation (Figure 13C).
- Polymetallic mineralisation crosscut by anhydrite ± chalcopyrite ± pyrite veins (Figure 13E).
- Porphyry D veins crosscut by anhydrite ± chalcopyrite veins (Figure 13E).
- Porphyry A veins crosscut by carbonate base-metal epithermal Au mineralisation (Figure 13I).

Multiple vein events of similar vein styles and reversals of the normal overprinting relationships provide valuable evidence of polyphasal emplacement of possibly blind porphyry intrusions which may contribute multiple events of mineralisation.

GEOCHEMISTRY

Multi-Element Whole Rock Analyses

A total of 124 drill core samples were submitted to ALS for analysis by the 'Complete Characterisation Package 1,' a whole rock litho-geochemistry technique involving a combination of lithium borate fusion, four acid digest and aqua regia digest sample preparations with ICP-AES and ICP-MS finish, for sixty-five elements. A selection of least-altered volcanic and intrusive rocks with minimal veins and mineralisation were chosen. The results were combined with whole rock XRF analyses by Crawford (2015). 'Least-altered' samples were chosen using the criteria (Loucks 2014): volatile-free major element oxides sum to 97.5-101.5 wt % and Loss On Ignition or H_2O+CO_2+S amounting to less than 3.5 wt %.

At Thursday's Gossan, the volcanic host rocks are low- to medium-K calc-alkaline dacite, andesite and basalt (Figure 14A). The majority of intrusive rocks plot in the subalkaline granodiorite, diorite and granite fields of a modified TAS diagram (Peccerillo and Taylor, 1976; Ewart, 1982)(Figure 14B). Most rock types from Thursday's Gossan have normal fractionation trends and the trace element signature of arc magmas; enrichment of K and Pb and depletion of Ti and Nb relative to mid-ocean ridge basalts (Figure 14C). The enrichment in Large Ion Lithophile elements was due to subduction of metasomatized mantle wedge. Samples of the HPMD plotted in the continental arc field of a Zr/Al_2O_3 versus $TiO2/Al_2O_3$ diagram and were enriched in P, Nd, Sm, Zr, Hf, Eu, Ti and Tb compared to all other rock types (Figure 14C), indicating magma from a heterogenous source region with a greater

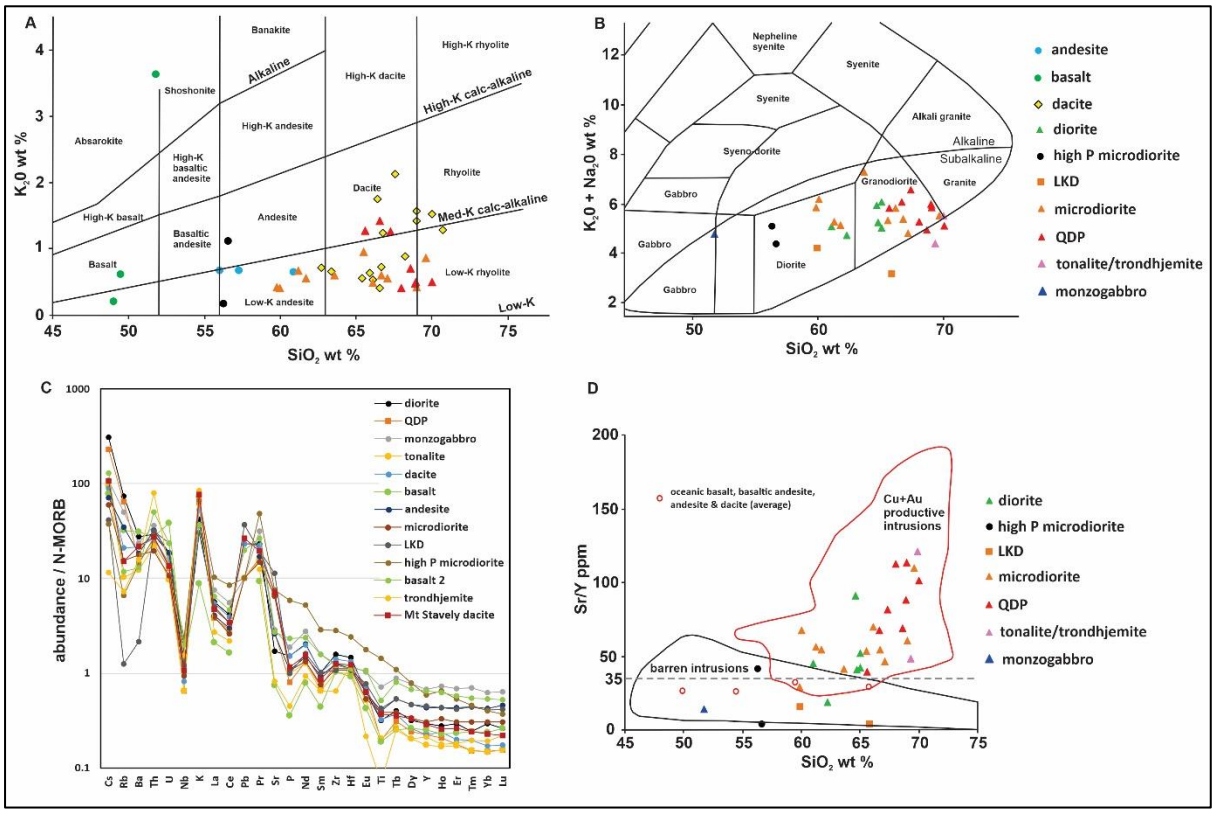

Figure 14. Major and trace element diagrams of least-altered volcanic and intrusive rock samples from Thursday's Gossan. A. K2O versus SiO2 plot of volcanics overlain by the fields of Ewart (1982). B. TAS diagram of intrusions with the fields of Peccerillo and Taylor (1976) and Ewart (1982). C. Spidergram of intrusive samples, normalised to the N-MORB values of Sun and McDonough (1989). D. Sr/Y versus SiO2 magma fertility plot with the fields from Loucks (2014).

component of high field strength element-enriched, metamorphosed mantle wedge or subducted oceanic crust (eg. Xiao et al, 2016).

Whole rock fertility indicators provide information about the water content and oxidation state of causative magmas. High Sr/Y ratios, >35 and high V/Sc ratios (Loucks 2014) result from fractional crystallisation of hornblende at the expense of plagioclase and titanomagnetite respectively. Apart from the HPMD and the later post-mineral Devonian LKD and younger MG intrusions, the Cambrian-age intrusive phases at Thursday's Gossan plot in the Cu+Au porphyry productive intrusion field of Loucks (2014) (Figure 14D). Samples of QDP and tonalite had the highest Sr/Y and V/Sc ratios, which indicates they were derived from relatively oxidised and hydrous magmas (Halley, 2016). In routine analyses, the V/Sc ratio >15 has been applied to represent the geochemical 'signature' of oxidised magmatic fluids responsible for hydrothermal metasomatism and mineralisation at Thursday's Gossan. The distribution of the >15 V/Sc ratio correlates well with the position of the 2200nm wavelength SWIR adsorption feature and observed polymetallic lode-style copper-gold-silver mineralisation (Figure 12) indicating a southward plunging hydrothermal system exists at Thursday's Gossan.

Sulphur Isotopes

A total of 218 sulphide and 12 sulphate samples from Thursday's Gossan were submitted to the Centre for Ore Deposit and Earth Sciences, University of Tasmania for measurement of sulphur isotopes. While most samples were from pyrite ± anhydrite D veins with sericite halos, a few were from hydrothermal breccias, chalcopyrite C/D veins and late carbonate and base metal veins. Pyrite, chalcopyrite, anhydrite and rarely bornite and chalcocite were extracted from diamond drill core, analysed and compared to the sulphur isotopic response of troylite in the Canyon Diablo meteorite (CDT). These analyses have been combined with the historical analysis for a total of 230 sulphur isotope analyses.

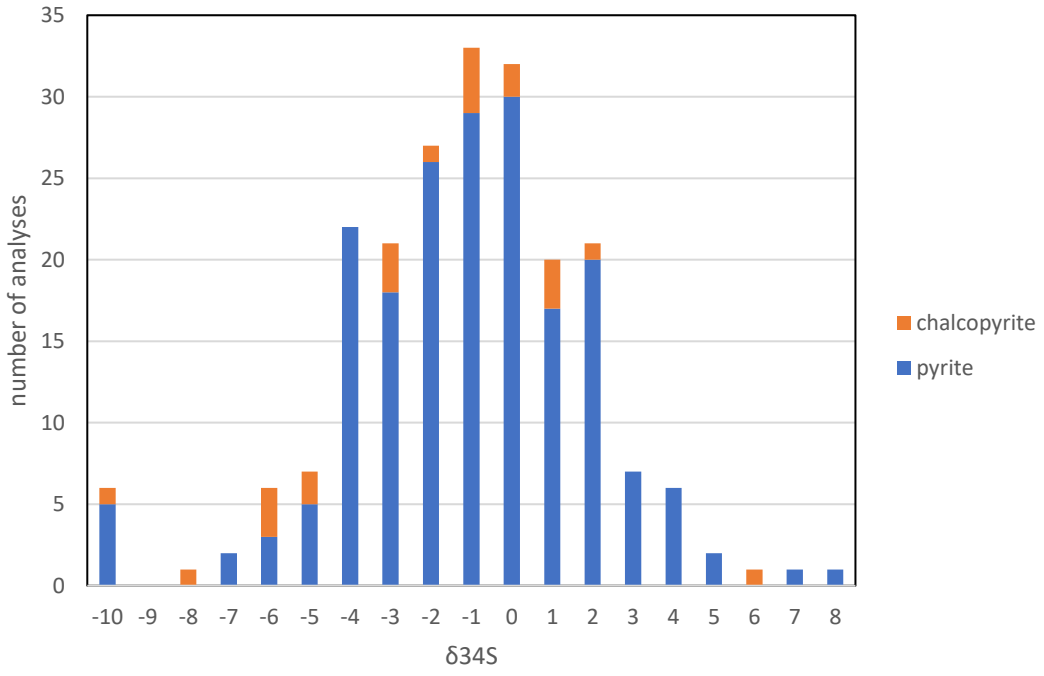

Figure 15. Frequency histogram showing distribution of δ34S values in pyrite and chalcopyrite.

Of the 218 suphide samples, 66 returned very light isotopic δ34S values of less than -3‰. This is effectively the threshold for light sulphur isotope results that correlates well with the copper-gold mineralisation at the Cadia Ridgeway Deposit near Orange, NSW (Wilson, 2003). Figure 15 and Table 1 summarises the range of δ34S values.

Mineral	N	Range of δ34S	Mean	Mode	Skew	STDEV
Py	194	-37.69 to 7.35‰	-1.83‰	-2.75‰	-4.01	4.30
Cp	22	-11.87 to 5.64‰	-2.79‰	-	-0.27	3.94
An	5	9.45 to 22.49‰	17.11‰	-	-0.63	4.41
Bn	1	-4.50‰	-	-	-	-
Ct	1	1.46‰	-	-	-	-

Table 1. Statistics for all Thursday's Gossan sulphur isotope analyses. Py = pyrite, Cp = chalcopyrite, An = anhydrite, Bn = bornite and Ct = chalcocite. N = number of analyses

The pyrite dominant samples returned a broad range of δ34S values, from -37.69 to 7.35‰ (Table 1). The chalcopyrite dominant samples ranged from -11.87 to 5.64‰. Anhydrite dominant samples had the heaviest sulphur isotopes, with δ34S values of 9.45 to 22.49‰. There was a negative skewness in the pyrite and chalcopyrite sulphur isotope values towards a lighter isotopic magmatic signature (Table 1). Pyrite, chalcopyrite and anhydrite δ34S results had similar standard deviations.

Late, low temperature carbonate ± base metal veins had the lightest pyrite sulphur isotopic signature, eg. -37.69‰ δ34S (SMD026, 747.0m) and -10.6‰ δ34S (SMD001, 154.0m). However, some carbonate veins returned positive δ34S pyrite values, eg. 0.01‰ (SMD031, 251.8m) and 7.35‰ (SMD028, 712.4m).

Excluding the carbonate ± base metal veins, the lightest isotopic / most negative δ34S values from pyrite and chalcopyrite occurred:

1) Within or immediately adjacent to the QDP intrusion and especially well correlated with the distribution of porphyry M veins (Figure 16)
2) Within or immediately adjacent to the NSS and CLS
3) In association with polymetallic epithermal assemblages at relatively shallow depths, on the UMC structure to the east

In contrast, pyrite D veins from the immediate footwall and hanging-wall of the LAS had weakly negative to moderately positive δ34S values. The results indicate that the moderately to steeply west-dipping NSS and CLS were conduits for the circulation of highly

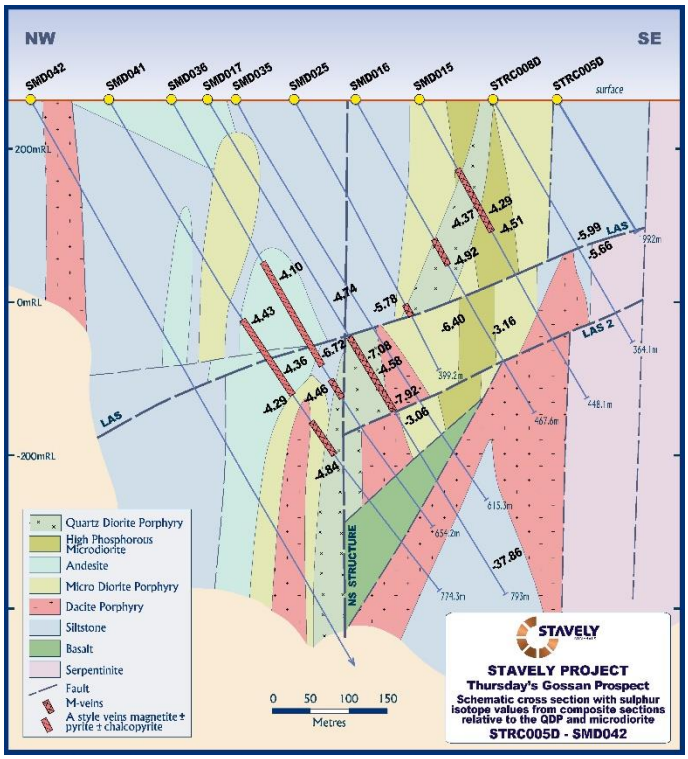

Figure 16. Drill section showing the distribution of light sulphur isotope results proximal to the QDP.

oxidised hydrothermal fluids rather than the Low Angle Structure and those oxidised hydrothermal fluids have overprinted the QDP intrusion. However, there were no systematic variations in δ34S values within/marginal to the QDP intrusion or the mineralised structures.

Pyrite-anhydrite and chalcopyrite-anhydrite veins were selected to estimate the formation temperature of the veins. The assumption was that the sulphide and sulphate co-precipitated in equilibrium. The relative timing relationships of anhydrite, pyrite and chalcopyrite remains speculative as there were multiple generations of anhydrite and gypsum and complex cross-cutting relationships. In places, anhydrite veins cut across pyrite veins and were themselves cut by pyrite veins. In other places, both anhydrite and pyrite appeared to co-exist in the one vein. The δ34S values from anhydrite were generally higher when associated with pyrite (11.33 to 23.21‰) than with chalcopyrite (9.45 to 17.76‰) (Table 2). The anhydrite-bearing veins are calculated to have formed at temperatures ranging from 248°C to 477°C while the highest temperatures occurred in the immediate hanging-wall of the NSS at depth.

Hole_ID	Depth	Sulphide	δ34S (sulphide)	Sulphate	δ34S (sulphate)	$\Delta_{sulphate-sulphide}$	Temp °C
SMD042	762.9	Py	2.45	An	15.99	13.54	410
SMD028	623.1	Py	1.03	An	19.45	18.42	309
SMD026	608.7	Py	-0.93	An	21.91	22.84	248
SMD029W1	600.25	Py	-3.15	An	17.97	21.12	270
SMD029W1	659.2	Py	1.92	An	13.25	11.33	477
SMD029W1	734.35	Py	-1.40	An	16.52	17.92	318
SMD044	671.8	Cp	-6.51	An	9.78	16.29	370
SMD044	755.3	Py	-0.72	An	22.49	23.21	244
SMD044	868.9	Py	0.02	An	18.65	18.63	306
SMD044	1024.75	Cp	-11.87	An	9.45	21.32	287
SMD044	1149.26	Cp	-1.56	An	17.76	19.32	316

Table 2. Temperatures of pyrite+anhydrite and chalcopyrite+anhydrite veins. Calculated using equations 12 and 15 in Seal (2006) and the fractionation factors from Ohmoto and Rye (1979) and Ohmoto and Lasage (1982). Py = pyrite, Cp = chalcopyrite and An = anhydrite.

DISCUSSION

There are both age dating and observational evidence of multiple phases of porphyry intrusion and overprinting alteration / mineralisation events at Thursday's Gossan. While the errors for age dates of the VTP and the QDP overlap, there is a strong suggestion that the VTP and its associated alteration assemblages / mineralisation are overprinted by the QDP porphyry and its associated alteration assemblages / mineralisation. The multiple alteration / mineralising events are partly demonstrated in drill hole SMD023 (Figure 17) where the EDP displays evidence of at least two alteration cycles (combined prograde and retrograde):

1. an early prograde potassium feldspar / pink albite wash in the groundmass
2. overprinted by retrograde sercite (phyllic) alteration of the groundmass (variable) and feldspars
3. cut by a prograde Early Dark Micaceous (EDM) vein
4. cut by an indistinct wormy porphyry A vein
5. cut by wispy porphyry M veins
6. cut by 'railroad track' porphyry M veins
7. cut by laminated porphyry M veins
8. Elsewhere, the porphyry M veins are cut by pyrite-chalcopyrite veinlets and transverse fracture fill

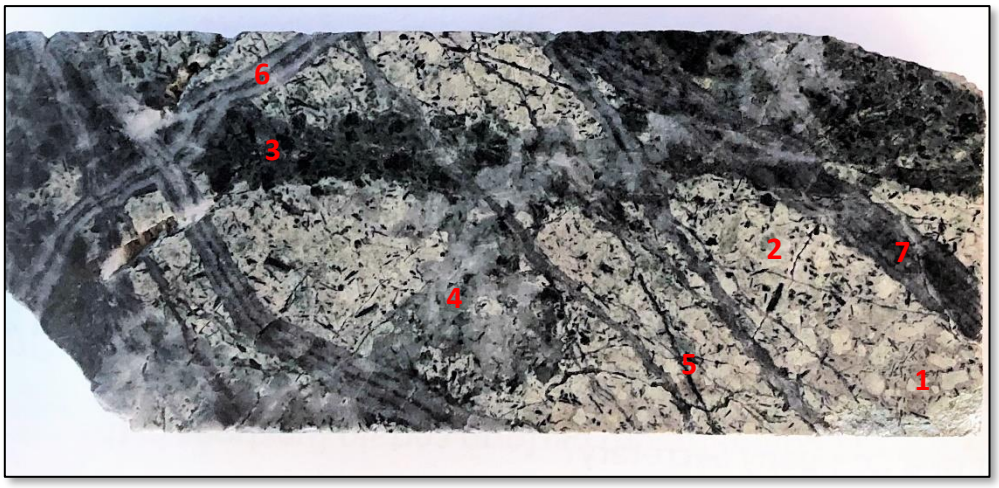

Figure 17. Half cut HQ drill core sample from 120m depth in SMD023 displaying multiphase sequence of alteration and veining in the EDP: 1) mushroom pink albite, 2) sericite alteration of feldspars, 3) EDM fracture vein selvages, 4) watery, wormy porphyry A veins, 5) wispy porphyry M veins, 6) 'railroad track' porphyry M veins, 7) laminated porphyry M veins.

The earlier prograde pink albite wash and the retrograde sericite alteration could be associated with the VTP while the next prograde phase of alteration and veining with the EDM veins, the wormy porphyry A vein and the wispy to laminated porphyry M veins all cross cut the earlier prograde / retrograde alteration assemblages. It is considered that the QDP itself is responsible for the intense porphyry M vein swarms hosted in the apical proportion of the QDP, on its margins and within host units the QDP intrudes including the HPMD and EDP. The porphyry M veins can be traced along individual veins as they morph into both watery / wormy porphyry A veins and also into aplite vein / dykes and this is taken as evidence of the veins being located near the top of the QDP intrusion.

The QDP and all other Early Porphyry and Inter-Mineral Porphyry intrusions are cut by late-stage quartz-pyrite porphyry D veins that are considered as evidence of the late mineralisation stage of an unseen Inferred Porphyry 1. The same structures hosting these late porphyry D veins from Inferred Porphyry 1 are re-opened during another prograde mineralising event that introduced the advanced argillic alteration assemblage (pyrophyllite, dickite and minor alunite) and structurally-controlled polymetallic copper sulphide mineralisation (enargite, tennantite, chalcocite, bornite, chalcopyrite with minor covellite and colusite) in and proximal to the CLS and NSS, and to a lesser extent the UMC structure. It is concluded that this prograde event must be emanating from another porphyry phase – the Inferred Porphyry 2.

The hotter prograde phases of alteration at Thursday's Gossan appear not to be the classic potassic alteration noted in many porphyry systems but rather is dominated by a sodic alteration assemblage similar to that at Namosi, Fiji (Orovan et al., 2018). Petrographic descriptions have noted rare relict early shreddy biotite prograde alteration of original mafic minerals (hornblende) overprinted by sericite and chlorite retrograde alteration (Ashley, 2018). A compiled sequence of intrusion, alteration and veining / mineralisation is presented in Figure 18.

The light sulphur isotope results and the high V/Sc ratios indicate that the mineralising fluids were sourced from a highly oxidised and hydrous melt with positive implications for the metal carrying capacity of the hydrothermal fluids and the mineralisation potential of the hydrothermal system at Thursday's Gossan (Halley, 2016).

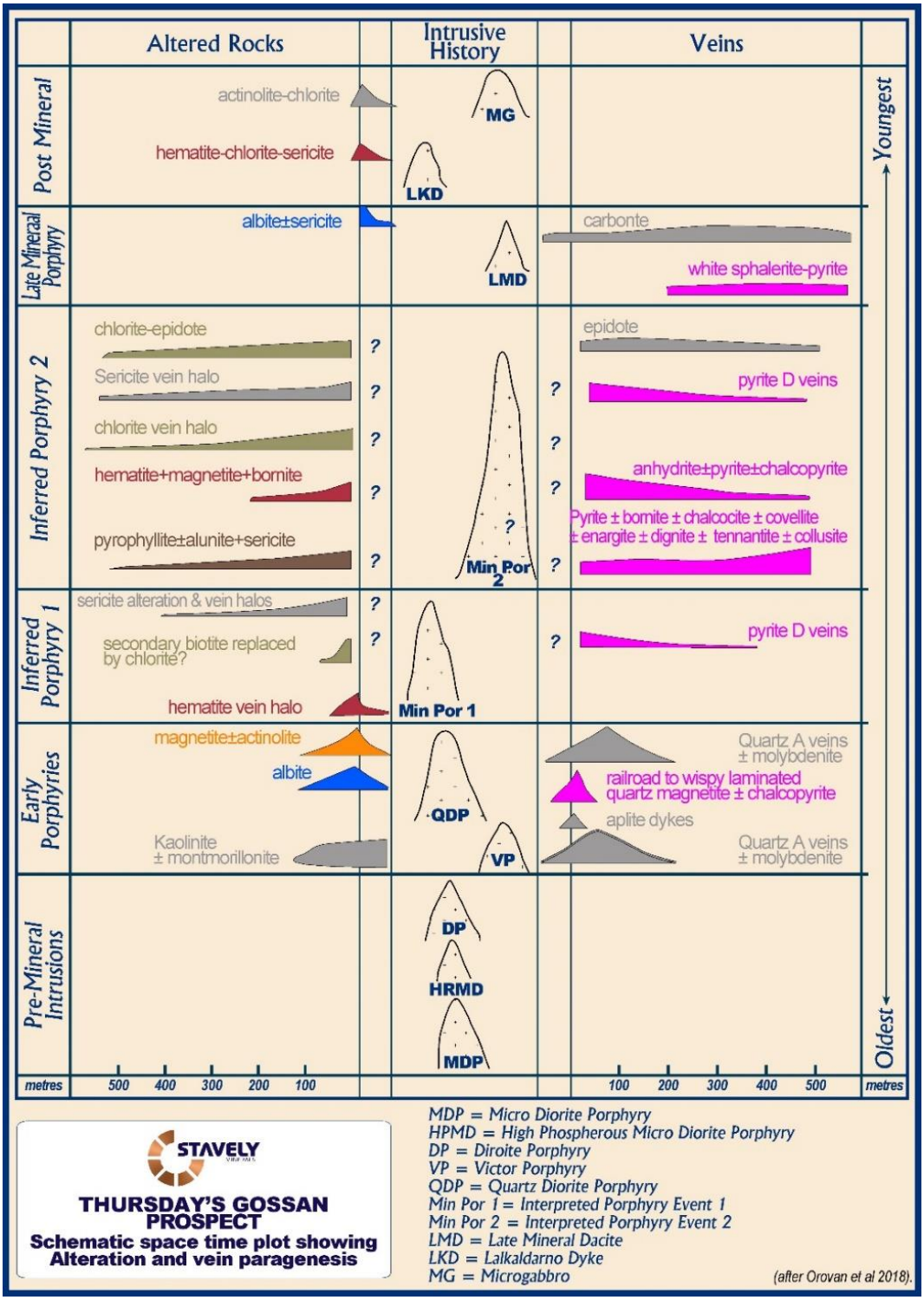

Figure 18. Schematic space time plot showing alteration and vein paragenesis at Thursday's Gossan after After Orovan et al 2018. The diagram depicts the oldest events at the bottom and the youngest at the top. The lateral extent of each black band indicates the distribution of the vein or alteration type observed in drill core relative to the related intrusive margin where known. The vertical bars directly adjacent to the intrusive history column indicate distribution within the porphyry intrusion.

The high-grade polymetallic lodes at Thursday's Gossan have distinct similarities to other noted vein copper deposits, including those at Magma, Arizona, Butte, Montana and Mt Lyell, Tasmania (Houston and Dilles 2013; Bartos 1989, Baumgartner et al. 2008; Hammer and Peterson 1968, Meyer et al. 1968) with the following common attributes:

- Structurally controlled mineralisation
- Association with faults, fault systems, vein breccia zones and replacement zones that accommodate both extension and shortening
- Occurrence of semi-massive to massive sulphide
- Mineral assemblages which reflect a high-sulphidation state and low pH
- Proximity to felsic porphyritic intrusions and possibly porphyry copper deposits (eg. Resolution)
- Superposition of Cu- and/or Zn-sulphides over pyrite-quartz bodies; multiple stages of mineralisation
- Mineral zonation from proximal Cu- to distal Zn+Pb-rich assemblages with distance from a heat / magmatic fluid source
- Long lived, multiphase mineralising systems with complex temporal overprints,
- Telescoping of veins formed under hydrostatic conditions, at shallow depths over porphyry veins formed under lithostatic conditions at greater depths due to regional shortening, uplift and erosion (eg. Butte).

Some of the best examples of 'lode-style' polymetallic epithermal deposits developed in proximity to porphyry centres include the Magma vein, Arizona (12.4Mt @ 5.69% Cu, 66g/t Ag and 1.1g/t Au (1911 to 1964 production; Hammer and Peterson, 1968), the Butte District, Montana (296Mt @ 2.5% Cu, 68g/t Ag and 0.3g/t Au (1880 to 1964 production; Meyer et al 1968), the Lepanto deposit, Philippines (36.3Mt @ 2.9% Cu, 14g/t Ag and 3.4g/t Au (1936 to1996 production; Hedenquest et al 2017) and Cerro De Pasco deposit, Peru (1,200Moz Ag, 2Moz Au and 50Mt @ 2% Cu; Baumbartner et al 2008), although the porphyry association with Cerro De Pasco remains to be demonstrated. These deposits have a paragenetic sequence of vein-filling sulphides that indicates prograde evolution of the fluid and a deep heat source (Kirkham and Sinclair 1996; Bartos 1989). Guilbert and Park (1986) noted that the thickness and grade of the veins reflected structurally controlled permeability, where dilation is enhanced by the intersection of cross-structures and by changes in the strike and dip of the faults. The 0.25m to 20m wide Magma vein had an upper sphalerite-rich zone, intermediate bornite bodies and lower zone containing enargite, together with pyrite and chalcopyrite (Guilbert and Park 1986; Short et al 1943). Ballyntine et al (2003) reported that bornite-chalcocite veins extended south of the Magma vein and cut across the top of the adjacent Resolution porphyry copper deposit (1.8Bt at 1.53% Cu - Rio Tinto Annual Report, 2018).

CONCLUSIONS

Recent mapping of sulphide species spatial distribution at Thursday's Gossan suggests a systematic zonation in Cu species within high-grade lode structures providing a potential vector towards a porphyry source. Recognition of the high-grade structurally-controlled copper-gold-silver mineralisation and its sulphide species zonation provides additional opportunities to pursue this style of mineralisation in the area in parallel and sympathetic structures, especially closer to surface.

The analogies of the Butte, Montana, Magma, Arizona and Mount Lyell, Tasmania mineral systems and a review of the extensive literature on those deposits has been very informative in understanding the hydrothermal mineralisation at Thursday's Gossan.

Many thanks are offered for the insights and many discussions provided by our primary consultants Dr Greg Corbett, Dr Scott Halley and Dr Paul Ashley.

REFERENCES

Arancibia, O. N. and Clark, A. H., 1996, Early magnetite-amphibole-plagioclase alteration-mineralization in the Island copper porphyry copper-gold-molybdenum deposit, British Columbia. Economic Geology, 91 (2); 402-438.

Ashley, P., 2017-2019, Petrographic Reports on Thursday's Gossan, various unpublished reports.

Bartos, P.J., 1989, Prograde and retrograde base metal lode deposits and their relationship to underlying porphyry copper deposits. Economic Geology, 84; 1671-1683.

Baumgartner, R., Fontbote, L. and Vennemann, T., 2008, Mineral Zoning, Geochemistry of Epithermal Polymetallic Zn-Pb-Ag-Cu-Bi Mineralization at Cerro de Pasco, Peru. Economic Geology 103, 493-537.

Bucher, M. unpublished Ar-Ar date for Lalkaldarno Porphyry in Stuart-Smith, P.G. and Black, L.P., 1999. Willaura, Sheet 7422, Victoria, 1:100 000 Map Geological Report. Australian Geological Survey Organisation, Record 1999/38.

Cairns, C., Menzies, D., Corbett, G., Forgan, H., and Murphy, J., 2015, The Thursday's Gossan – it can't run but it can hide. Mines and Wines 2015, Discoveries in The Tasmanides, The Australian Institute Of Geoscientists, Bulletin 67, 3-4 September, 2015 Orange, NSW. 13p.

Cayley, R., Lewis, C., Taylor, D., Schofield, A., Skladzien, P., and Cairns, C., 2018, 2.1 Basement geology. In: Schofield A. Ed., Regional geology and mineral systems of the Stavely Arc, western Victoria. Geoscience Australia, Record 2018/02, p. 18-38.

Cayley, R.A., McLean, M.A., Skladzien, P.B and Cairns, C.P., 2018, Stavely project regional 3D geological model. Stavely Project Report 3. Geological Survey of Victoria. Department of Economic Development, Jobs, Transport and Resources. 259p.

Corbett, G.J., 2017, Epithermal Au-Ag and porphyry Cu-Au exploration – Short Course Manual: unpublished., www.corbettgeology.com

Corbett, G. 2018, Comments on the recent drill program at Stavely Porphyry Cu Project, Victoria, an unpublished internal company report.

Corbett, G., 2019a, Comments on the significance of Diamond Drill Hole SMD044 at the Stavely Porphyry Cu-Au Project, Western Victoria, Australia, an unpublished internal company report.

Corbett, G.J., 2019b, Time in porphyry Cu-Au Development – exploration implications: PACRIM, Mineral Systems of the Pacific Rim Congress. The Australasian Institute of Mining and Metallurgy, Auckland, 3-5 April, 2019.

Crawford, A.J., 2015, Petrographic Report. 9 rocks from the Stavely porphyry-Cu project, Western Victoria. Unpublished exploration report for Anglo American Exploration (Perth). A & A Crawford Geological Research Consultants. 40p.

Guilbert, J.M. and Park Jr, C.F., 1986, The geology of ore deposits. Waveland Press Inc., Illinois. 985p.

Gustafson, L.B. and Hunt, J.P.,1975, The Porphyry Copper Deposit at El Salvador, Chile. Economic Geology, 70, 857-912.

Halley, S., Dilles, J., Tosdal, R., 2015, Footprints: hydrothermal alteration and geochemical dispersion around Porphyry Copper Deposits, SEG newsletter Jan 2015, 100; 1, and 12-17.

Halley, S, 2019, Thursday's Gossan, Classification of rock compositions and gangue mineralogy from assay and spectral data, Internal company report.

Hammer, D. F., and Peterson, D. W., 1968, Geology of the Magma mine area, Arizona, in Ridge, J. D., ed., Ore deposits of the United States, 1933-1967 (Graton-Sales Volume): New York, American Institute of Mining, Metallurgical, and Petroleum Engineers, v. 2, p. 1282-1310.

Hedenquest, J.W., Arribas, R., R., and Aoki, M., 2017, Zonation of sulfate and sulfide minerals and isotopic composition in the Far Southeast porphyry and Lepanto epithermal Cu–Au deposits, Philippines. Resource Geology, 67; 174-196.

Houston, R.A, and Dilles, J.H., 2013, Structural geologic evolution of the Butte District, Montana. Economic Geology, 108, 1397-1424.

Kirkham, R.V., and Sinclair, W.D. 1996, 17. Vein copper. In: Eckstrand O.R., Sinclair W.R. and Thorpe R.I eds, Geology of Canadian Mineral Deposit Types, Geological Survey of Canada, 8, 399-408.

Le Maitre, R.W., (editor), A. Streckeisen, B. Zanettin, M. J. Le Bas, B. Bonin, P. Bateman, G. Bellieni, A. Dudek, S. Efremova, J. Keller, J. Lamere, P. A. Sabine, R. Schmid, H. Sorensen, and A. R. Woolley, Igneous Rocks: A Classification and Glossary of Terms, Recommendations of the International Union of Geological Sciences, Subcommission of the Systematics of Igneous Rocks. Cambridge University Press, 2002.

Lewis, C.J., Taylor, D., Cayley, R.A., Schofield, A. and Skladzien, P.B. 2015, New SHRIMP U-Pb zircon ages from the Stavely region, western Victoria: July 2013-June2014. Record 2015/26. Geoscience Australia, Canberra.

Lewis, C.J., Cayley, R.A., Duncan, R.J., Schofield, A. and Taylor, D.H. 2016, New SHRIMP U-Pb zircon ages from the Stavely region, western Victoria: July 2014-June 2016. Record 2016/27. Geoscience Australia, Canberra.

Lickfold, V.,2002, Intrusive history and volatile evolution of Endeavour porphyry Cu-Au deposits, Goonumbla district, NSW, Australia, Unpublished PhD thesis, University of Tasmania. 245p.

Loucks, R.R. 2014, Distinctive composition of copper ore-forming arc magmas: Australian Journal of Earth Sciences, v. 61, p. 5-16.

Meyer, C., Shea, E. P., Goddard, C. C., Jr., and staff, 1968, Ore deposits at Butte, Montana, in Ridge, J. D., ed., Ore deposits of the United States, 1933-1967 (Graton-Sales Volume): New York, American Institute of Mining, Metallurgical, and Petroleum Engineers, v. 2, p. 1373-1416.

Norman, M., 2014, Re-Os isotope dating of molybdenite from southeastern Australia. Report to Geoscience Australia. Research School of Earth Sciences. Australian National University (unpublished).

Norman, M., 2015, Re-Os isotope dating of molybdenite from southeastern Australia: update. Report to Geoscience Australia. Research School of Earth Sciences. Australian National University (unpublished).

Ohmoto, H. and Rye, R.O., 1979. Isotopes of sulfur and carbon. In: Geochemistry of Hydrothermal Ore Deposits. Barnes HL (ed) J Wiley and Sons, p 509-567.

Ohmoto, H. and Lasaga, A.C., 1982, Kinetics of reactions between aqueous sulfates and sulfides in hydrothermal systems. Geochimica Cosmochimica Acta 46:1727-1745.

Orovan, E., Cooke, D., Harris, A., Ackerman, B. and Lawlis, E. 2018, Geology and isotope geochemistry of the Wainaulo Cu-Au porphyry deposit, Namosi District, Fiji: Economic Geology v. 113, pp 133-161

Peccerillo, A., and Taylor, S. R., 1976, Geochemistry of Eocene calc-alkaline volcanic rocks from the Kastamonu area, northern Turkey: Contributions to Mineralogy and Petrology, v. 58, p. 63-81.

Ransome, F.L., 1912, Copper Deposits Near Superior, Arizona. Contributions to Economic Geology, Part 1., pp. 139-158.

Schofield, A., (ed.) 2018, Regional geology and mineral systems of the Stavely Arc, western Victoria. Record 2018/02. Geoscience Australia, Canberra.

Schofield, A., McAlpine, S., and Bailey A., 2018, 2.6 Geochemistry of the Stavely Arc. In: Schofield A. Ed., Regional geology and mineral systems of the Stavely Arc, western Victoria. Geoscience Australia, Record 2018/02, p. 101-134.

Seal, R.R, 2006, Sulfur Isotope Geochemistry of Sulfide Minerals. Reviews in Mineralogy and Geochemistry, Geological Society of America 61:633-677.

Short, M.N., Galbraith, F.W., Harshman, E.N., Kuhn, T.H., and Wilson, D., 1943, Geology of the ore deposits of the Superior mining area, Arizona. Arizona Bureau of Mines, Geological Series 16, Bulletin 151, October 1943. 159p.

Sinclair, W.D., 2007, Porphyry deposits, in Goodfellow, W.D., ed., Mineral Deposits of Canada: A Synthesis of Major Deposit-Types, District Metallogeny, the Evolution of Geological Provinces, and Exploration Methods: Geological Association of Canada, Mineral Deposits Division, Special Publication No. 5, p. 223-243.

Sillitoe, R., 2010, Porphyry Copper Systems. Economic Geology; 105 (1): 3–41

Sillitoe, R., 2000, Gold-Rich Porphyry Deposits: Descriptive and Genetic Models and Their Role in Exploration and Discovery, SEG Reviews, Vol. 13, pp. 315-345.

Spencer, A.A.S, 1996, Geology, Mineralisation and Hydrothermal Alteration Of Thursday's Gossan Porphyry System, Stavely, Western Victoria. Honours Thesis, La Trobe University, Melbourne, 96pp. (unpublished).

Stanley, C. R., and Madeisky, H. E., 1996, Lithogeochemical exploration for metasomatic zones associated with hydrothermal mineral deposits using Pearce Element Ratio Analysis. Short course notes on Pearce Element Ration Analysis, Mineral Deposit Research Unit. pp. 99.

Stuart-Smith, P.G., and Black, L.P. 1999, Wialura Sheet 7422, Victoria, 1:100,000 map geological report. Australian Geological Survey Organisation, Record 1999/38. 50p.

Sun, S. S., and McDonough, W. F., 1989, Chemical and isotopic systematics of oceanic basalts: implications for mantle composition and processes, *in* Saunders, A. D., and Norry, M. J., eds., Magmatism in Ocean Basins, London, Geological Society of London, Special Publication 42, p. 313-345.

Wilson, A.J., 2003, The geology, genesis and exploration context of the Cadia gold-copper porphyry deposits, New South Wales, Australia, Unpublished PhD thesis, University of Tasmania. 335p.

Xiao Y., Niu Y., Wan K-L., Lee D-C. and Iizuka Y., 2016. Geochemical behaviours of chemical elements during subduction-zone metamorphism and geodynamic significance. International Geology Review, 58, 1253-1277.

APPENDIX 1

U-Pb and Re-Os Geochronology of the Stavely Volcanic Arc and Thursday's Gossan

A suite of intrusions and molybdenite-mineralised quartz A veins were selected by Stavely Minerals for geochronology. Ten drill core samples of intrusions were submitted to the University of Tasmania for U-Pb dating of zircons using laser ICP-MS and combined with two age dates from Professor Tony Crawford in 2015 (unpublished data). Two examples of quartz-molybdenite A veins, one kilometre apart, were selected for high precision Re-Os dating of molybdenite using the "double-spike" method at the University of Alberta. The results of this work were combined with published age dates from Geoscience Australia and the Geological Survey of Victoria (Scofield et al., 2018) (Figure 13).

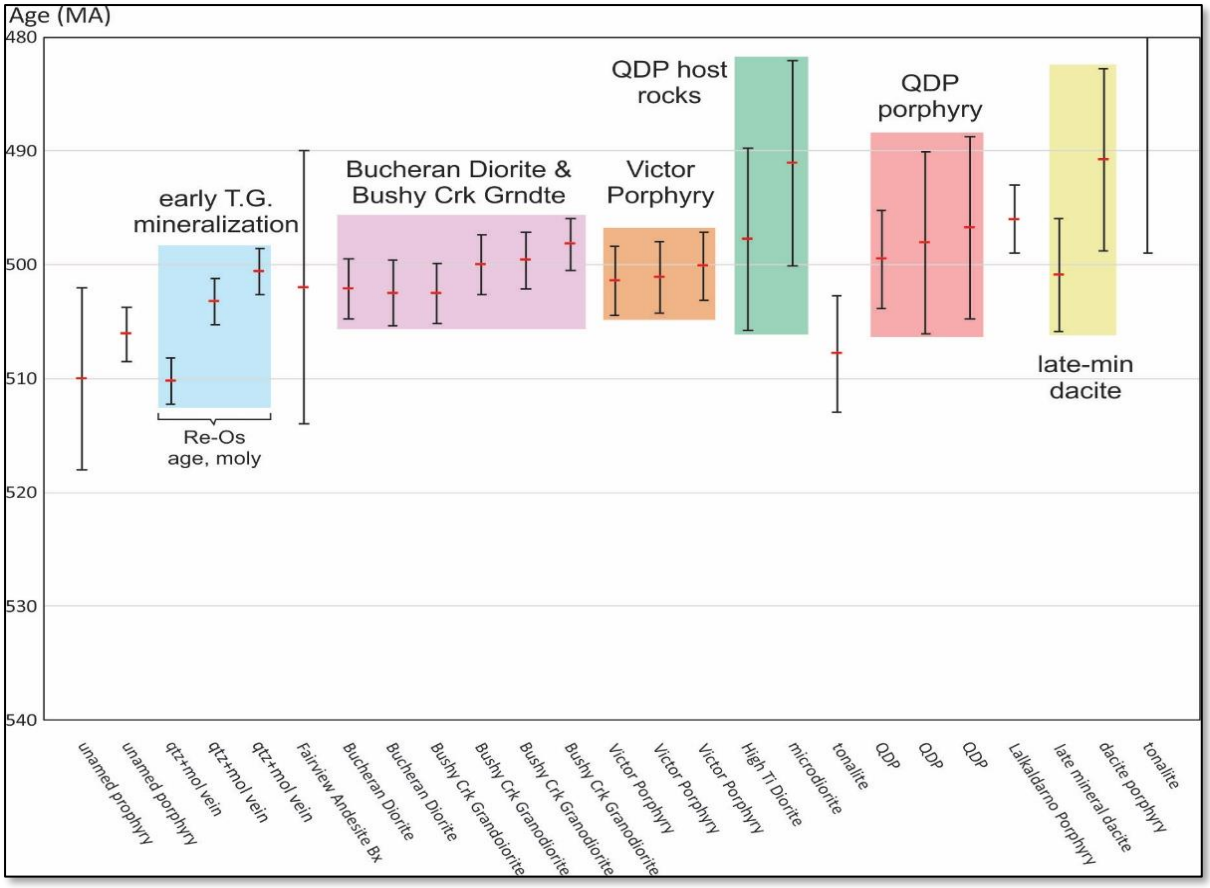

Figure 7. Summary of geochronology from Thursday's Gossan and the surrounding Stavely Belt with errors. All ages were derived from U-Pb isotopic ratios in zircons, except where indicated. A compilation of data from Stavely Minerals (2018, 2019), Norman (2014, 2015), Lewis et al (2015, 2016) and Bucher (unpublished Ar-Ar date presented in Stuart-Smith and Black, 1999).

The oldest rocks in the sequence are the Williamsons Road Serpentinite (WRS). While direct age dating has not been completed on this unit, the GSV consider the WRS to be geochemically identical to, and interpreted to be contemporaneous with, the Hummocks serpentinite (Scofield et al., 2018). The original relationships can be inferred in the western Glenelg Zone, where the Hummocks Serpentinite has a 'model' Sn/Nd age of ~'700' Ma with large errors, but, critically, appears to unconformably underlie sediments intruded by sills that are now SHRIMP dated at more than 600Ma. Consequently, the Hummocks Serpentinite in the Glenelg Zone context must be older than 600Ma, and based on equivalency, the WRS is considered older than 600Ma (Cayley, R. pers comm., 2019).

The Glenthompson Sandstone U/Pb dates on zircons provides a maximum age of deposition in four determinations of 569.0 ± 3.6Ma, 560.9 ± 4.2Ma, 552 ± 8Ma and 538 ± 23Ma (Lewis et al., 2016).

An unnamed porphyry intersected in drill hole STAVELY 17 (located some 10km south of Thursday's Gossan and drilled as part of the Stavely Arc project by Geoscience Australia and the Geology Survey of Victoria) returned U/Pb age dates from a small number of recovered zircons (n=4 and n=5) yielding circa 560Ma dates while another unnamed porphyry in the same drill hole returned an age date of 510 ± 8Ma, likewise from only 2 determinations (Scofield et al., 2018).

The oldest intrusive reasonably reliably dated in the Stavely Arc is a felsic intrusion into the WRS which returned a U/Pb zircon age date of 511.3 ± 2.9Ma. (Lewis et al., 2015)

In combination with intrusion U/Pb zircon age dates summarised by Lewis et al. (2016), the Thursday's Gossan volcano-sedimentary host rocks are broadly contemporaneous with the Early Porphyry VTP (504.4 ± 2.6Ma to 500.1 ± 3.0Ma), the Buckeran Diorite (502.1 ± 2.9Ma to 501.8 ± 2.6Ma), the Bushy Creek Granodiorite (502.5 ± 2.6Ma to 498.2 ± 2.3Ma), the Fairview Andesite Breccia (502 ± 12Ma), the Narrapumelap Road Dacite (503.2 ± 2.3Ma) and the Towanway Tuff (503.9 ±4.2Ma).

A slightly younger SHRIMP U/Pb zircon age date of 489 ± 7Ma from the Bushy Creek Granodiorite was determined by Black (1999).

Another sample in the Pre-Mineral Intrusion HPMD intrusion returned a date of 506.1 ± 2.4Ma. This intrusion also hosted a quartz vein with molybdenite that was dated by Re/Os at 510.2 ± 2.0Ma however, this determination was based on a single small grain of molybdenite considered to have introduced additional 'unquantifiable uncertainty' to the accuracy of the date (Norman, 2014 & 2015).

The Pre-Mineral Intrusion phase HPMD and MDP host rocks returned recent age dates of 497.8 ± 8.0Ma and 491.1 ± 9.0Ma respectively. These dates could be interpreted to indicate that the VTP is contemporaneous with the Bushy Creek Granodiorite and Buckeran Diorite while the Pre-Mineral Intrusions, the Early Porphyry and Inter-Mineral Porphyries at Thursday's Gossan represent a later phase of intrusion and mineralisation.

Two Dacite porphyry samples from Thursday's Gossan returned different dates; 507.8 ± 4.3 Ma. This age is similar to the age of the host sequence and also similar to the HPMD date described above, but the unit is considered to be the Early Dacite Porphyry – EDP. Another date of 475.6 ± 4.4 Ma is not supported by any other dating, is considered potentially unreliable and this specific data needs to be reviewed by an expert.

The Early Porphyry phases include the QDP, which intrudes the HPMD, MDP and EDP which has returned dates spanning 499.5 ± 4.3 Ma to 496.7 ± 8.0 Ma – the dating errors overlap and are considered to agree with observed intrusive relationships with respect to the Pre-Mineral Intrusions.

The LMD and LDP units intrude the QDP and were dated at 500.9 ± 5.0 Ma and 490.8 ± 8.0 Ma respectively. Again, the errors to these dates overlap but the median age of the two dates is materially different and highlights the challenges of age dating versus observed field relationships. The younger date accords with observed field relationships.

Lalkaldarno Regional Porphyry (496.0 ± 3.0 Ma) is observed as unaltered and unmineralized, has intruded to the ESE of the Victor porphyry and is considered amongst the last of the Cambrian-aged intrusions.

The LKD dyke, hosted within the re-activated LAS is Devonian-age and extends from 409.8 ± 7.0 Ma to 406.4 ± 4.1 Ma. The Microgabbro dyke(s) are observed intruding the LKD dyke.

Stavely Minerals had two molybdenite samples recently analysed at the University of Alberta, from SMD026 in the north and SMD008 in south, spatially approximately 1km apart, returning identical ages of 504.9±2.2 Ma.

In conjunction with mineralisation age dates previously obtained by Geoscience Australia (Norman, 2014 & 2015) the molybdenite ages indicate three possibly overlapping episodes of mineralisation:

1. 510.2 ± 2.0 Ma (this age of "unquantifiable uncertainty", especially given the younger 506.1 ± 2.4Ma age of the host intrusion),
2. 504.9 ± 2.2 Ma (2 of), 503.2 ± 2.0Ma, and
3. 500.6 ± 2.0 Ma.

Notably, all the Re/Os molybdenite ages pre-date the emplacement of the QDP. This apparent contradiction between the U/Pb dates of the host rocks and the Re-Os dates of the mineralisation is not unique to Thursday's Gossan and may represent a systematic bias in the two geochronology techniques seen elsewhere including the Lachlan Fold Belt (Harris, A., pers comm.).

It is possible that the circa 504Ma and 500Ma dates are reflecting two different phases of mineralisation. This may be reflecting an early mineralisation phase associated with the VTP and a later phase of mineralisation associated with the QDP and Inferred Porphyries 1 & 2. More work needs to be done to clarify this timing relationship.

A compilation of intrusion age dates is presented in Figure 7.